ORNL/TM-6706

ornl

OAK RIDGE NATIONAL LABORATORY

UNION CARBIDE

A Mathematical Model for Multicomponent Separations on the Continuous Annular Chromatograph

Robert L. Bratzler
John M. Begovich

OPERATED BY
UNION CARBIDE CORPORATION
FOR THE UNITED STATES
DEPARTMENT OF ENERGY

DISCLAIMER

Printed in the United States of America. Available from
National Technical Information Service
U.S. Department of Commerce
5285 Port Royal Road, Springfield, Virginia 22161
NTIS price codes—Printed Copy: A05; Microfiche A01

ORNL/TM-6706

Contract No. W-7405-eng-26

CHEMICAL TECHNOLOGY DIVISION

A MATHEMATICAL MODEL FOR MULTICOMPONENT SEPARATIONS ON THE CONTINUOUS ANNULAR CHROMATOGRAPH

Robert L. Bratzler*
John M. Begovich

*Present address: Polaroid Corporation, Cambridge, Massachusetts 02139

Date Published - December 1980

OAK RIDGE NATIONAL LABORATORY
Oak Ridge, Tennessee 37830
operated by
UNION CARBIDE CORPORATION
for the
DEPARTMENT OF ENERGY

THIS PAGE

WAS INTENTIONALLY

LEFT BLANK

CONTENTS

A MATHEMATICAL MODEL FOR MULTICOMPONENT SEPARATIONS ON THE CONTINUOUS ANNULAR CHROMATOGRAPH

Robert L. Bratzler
John M. Begovich

HIGHLIGHTS

A model for multicomponent separations on ion exchange columns has been adapted for use in studying the performance of the continuous annular chromatograph. The model accurately predicts solute peak positions in the column effluent and qualitatively predicts trends in solute effluent resolution as a function of increasing bandwidth of the solute feed pulse. The major virtues of the model are its simplicity in terms of the calculations involved and the fact that it incorporates the nonlinear solute–resin binding isotherms common in many ion exchange separations. Because dispersion effects are not accounted for in the model, discrepancies exist between the shapes of the effluent peaks predicted by the model and those determined experimentally.

---

1. INTRODUCTION

Conventional chromatographic separations have been modeled using both numerical and analytical calculations. Only the numerical methods have been successful in incorporating all of the effects which occur in chromatography. Unfortunately, the calculations are usually long and involved and do not yield much insight into the physics of the process. On the other hand, the analytical methods usually involve assumptions which yield only approximate results of the real experiment. However, they do provide a theoretical basis for predicting the results of a chromatographic separation with fewer calculations than with the numerical methods.

If the discussion is restricted to analytical models developed by ion exchange chromatographic separations, it must include the following effects in the most general model: (1) solute and solvent convection axially through the bed (column); (2) solute dispersion and diffusion, both parallel and normal to the direction of flow; and (3) nonlinear sorption and desorption of the solute by the bed packing. To date no analytical model has been developed which includes all of these effects. A model does exist for unidimensional convection and dispersion with linear binding isotherms.[1] This model is adequate for those instances in which the concentrations of solutes are much smaller than the concentrations at which the bed packing would be saturated (overloaded). For those cases in which the solute loading is relatively high, an analytical model has been developed by Rhee[2] which treats nonlinear solute binding isotherms, but it does not include diffusion and dispersion effects. Others[3] have developed models based on the idea that the column may be approximated as a number of ideal mixing cells, all connected in series. Although this approach is based on relatively crude geometrical assumptions, the results predicted have been shown to agree fairly well with experimental findings, provided the bed is sufficiently long.

Both cell models[4] and numerical models[5] have been employed in describing the continuous annular chromatograph (CAC) developed at the Oak Ridge National Laboratory. A schematic diagram of the apparatus is shown in Fig. 1. A regulated gas overpressure provides the driving force for a constant flow rate of eluent through the column. The feed inlet is held stationary while the column is rotated, subjecting each portion of the annulus to feed for a short period of time followed by

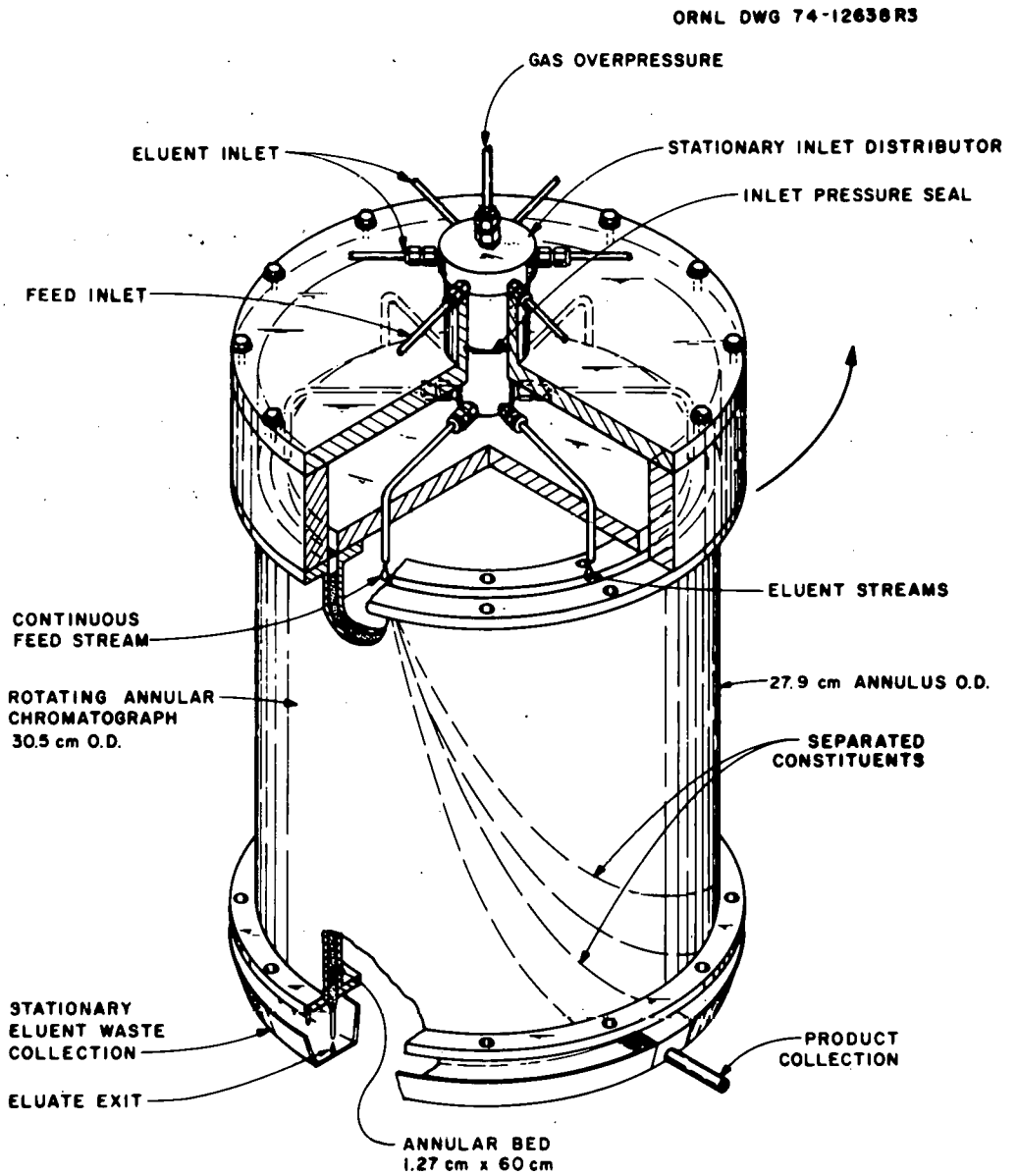

Fig. 1. Schematic of the pressurized continuous annular chromatograph.

elution by the eluent stream. As elution proceeds, the eluted substances separate as they progress vertically down the annulus, giving the appearance of helices as the annulus rotates. Component species with a high affinity for the column packing exit from the rotating annulus at a greater distance from the feed point compared to species with lower distribution coefficients. Thus, multicomponent separations can be made on a continuous basis depending on the sorption characteristics of the component species.

The purpose of the work reported here is to assess the applicability of the Rhee analytical model to the performance of the CAC. The following sections describe the model, and the results predicted by the model are compared with experimental results.

2. SUMMARY OF THE ANALYTICAL MODEL

Consider a conventional chromatographic column to which a liquid solute mixture is fed for some short-time interval, t_p, and is followed by a stream containing just solvent (the eluent stream). If there is sufficient variation in the affinities of the individual solutes for the column packing material, the solutes will appear separated in the effluent stream. The governing partial differential material balance on the column is:

$$D_i \frac{\partial^2 C_i}{\partial x^2} - \frac{v}{\varepsilon} \frac{\partial C_i}{\partial x} = \frac{\partial C_i}{\partial t} + \frac{(1-\varepsilon)}{\varepsilon} \frac{\partial B_i}{\partial t} \qquad (1)$$

$$\frac{\partial B_i}{\partial t} = k_{fi} C_i (N - \sum_{j=1}^{n} B_j) - k_{ri} B_i \ , \qquad (2)$$

where the nomenclature used is given in Table 1. Equation (1) results from a material balance performed on the mobile (liquid) phase, whereas Eq. (2) applies to the immobile (solid) phase. These equations are general and cannot be solved without simplifying the assumptions and specifying the initial and boundary conditions. For the case considered here, these latter conditions are:

$$t = 0, \text{ all } x: \quad C_i = B_i = 0 \tag{3}$$

$$0 < t \leq t_p, \; x = 0: \quad C_i = C_{io}$$

$$t > t_p, \; x = 0: \quad C_i = 0$$

$$\lim_{x \to \infty} C_i = 0$$

Thus, the column is initially free of solute; up to time, t_p, the column feed contains solute of some constant concentration; thereafter, solute-free eluent is fed to the column. Neglecting column end effects, it is assumed that the concentration vanishes as the axial position approaches infinity.

The model is simplified by neglecting the second-order dispersion terms in Eq. (1). A second simplification is to assume that the binding reaction [Eq. (2)] is sufficiently fast so that local chemical equilibrium exists throughout the column. This second assumption is valid in most cases, because the flow rates through ion exchange columns are relatively slow and the binding reactions are quite fast. The first assumption is made, not from physical insight, but rather to facilitate an analytical solution to the problem. Indeed, dispersion effects play a large role in determining the performance of chromatographic separations.

Table 1. Nomenclature

Symbol	Definition and units
B_i	Concentration of solute i bound to resin, meq/ml resin
C_i	Concentration of solute i in liquid phase, meq/ml solution
C_{io}	Concentration of solute i in liquid feed, meq/ml solution
D_i	Dispersion coefficient for solute i, cm^2/sec
k_{fi}	Forward binding-rate constant for solute i, (ml solution)/(sec-meq)
k_{ri}	Reverse binding-rate constant for solute i, sec^{-1}
K_i	k_{fi}/k_{ri} = binding constant, ml solution/meq
L	Overall bed length, cm
N	Resin capacity, meq/ml resin
n	Number of solutes in system
t_p	Duration of solute feed pulse, sec
t	Time, h
v	Eluent superficial velocity, cm/min
x	Axial coordinate, cm
ε	Bed void fraction, ml voids/ml bed
θ	Angular displacement, deg arc
Φ_i	K_iC_i, dimensionless transformed solute i concentration
ω	Annular bed rotation rate, deg arc/h

Even with these simplifying assumptions, Eqs. (1) and (2) are difficult to solve because of the nonlinearity in the concentration terms in Eq. (2). For instantaneous binding, Eq. (2) may be rearranged into the following form:

$$B_i = \frac{K_i N C_i}{1 + \sum_{j=1}^{n} K_j C_j} . \tag{4}$$

This equation is often called the Langmuir binding isotherm. A plot of this function is shown in Fig. 2. It adequately describes the "saturability" of the ion exchange resin as the concentration of solute in the mobile phase is increased. This equation is based on the concept that the resin has only a finite number of binding sites. As sites become filled, the tendency of any particular solute to bind decreases. This is an important consideration in the description of multicomponent chromatography, because the presence of a solute with a higher affinity for the resin will effectively displace solutes with lower resin affinities. The linear binding model described in ref. 1 does not include this effect.

The problem as posed has been solved analytically.[2] To apply the solution to the CAC, in which solute bands are distributed both axially and circumferentially, only a simple transformation from time to circumferential displacement is needed:

$$\theta = \omega t . \tag{5}$$

Thus, these two coordinates may be viewed as interchangeable.

The solution to the problem is best understood from plots in the x-t (or x-θ) plane. Consider the separation of a three-component mixture (three solutes plus solvent). For clarity, the solutes are numbered in

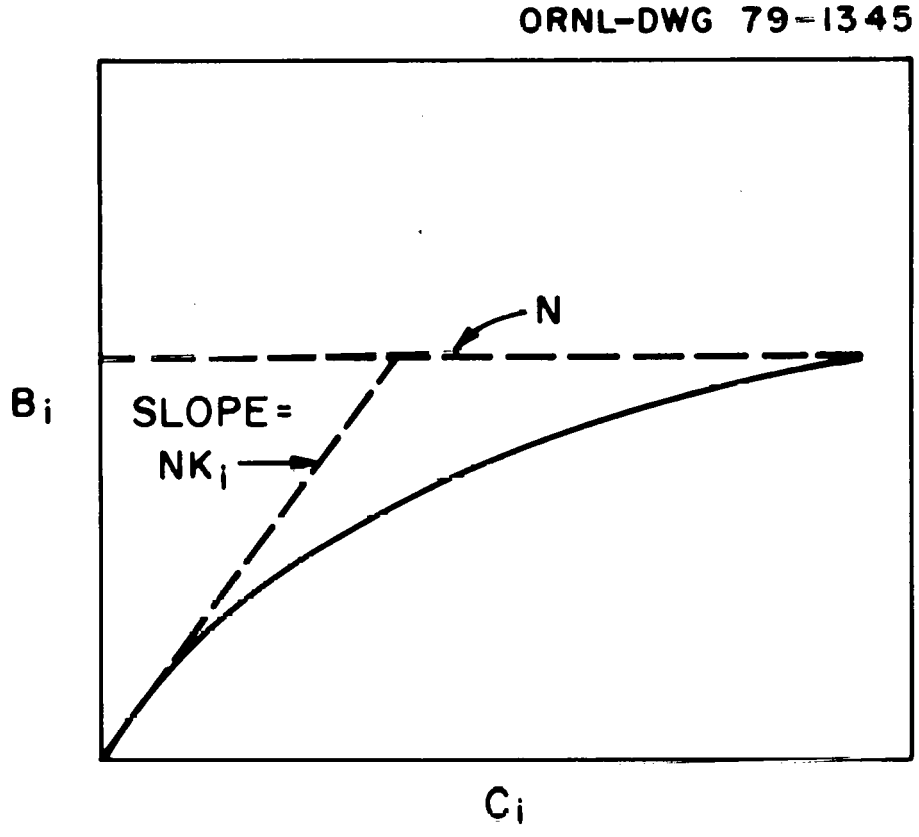

Fig. 2. Langmuir isotherm.

the order of increasing affinity for the resin, solute 1 having the lowest affinity and solute 3 having the highest. Because solute 3 will spend a greater proportion of time on the immobile phase, it will advance through the column at a slower rate than solutes 1 and 2. Thus if the column is initially solute-free when the mixture is applied ($t = 0$), a series of shock waves, one for each solute, will be established which demarcate the position of the solute fronts in the column. This is shown in Fig. 3. The solute fronts are sharp (i.e., the shock fronts) because dispersion has been neglected. Solute 1 front advances the fastest. The numbers of Fig. 3 indicate the solute content in the front and trailing regions near each of the three shock waves. To the left of shock 3, all three solutes coexist at concentrations equal to the respective feed concentrations. To the right of shock 3, only solutes 1 and 2 are present, and to the right of shock 2, only solute 1 exists.

At some later time, t_p, the column feed is switched to pure solvent, and elution of the column begins. Because the solvent does not interact with the resin, it will advance through the column faster than any of the solutes. Solute that resides on the resin will be removed progressively, starting with solute 1 (the solute with the lowest affinity for the resin). Thus, the mobile phase concentration of solute 1 will gradually decrease from its maximum value (= the inlet feed concentration) to zero. Graphically, this is represented by a fan of isoconcentration lines originating at $(0,t_p)$ as shown in Fig. 4. This family of lines may be regarded as the solvent front permeating the column.

There will be as many fans as there are solutes in the column, in this case, three. The fan for solute 1 will have smallest slopes (because

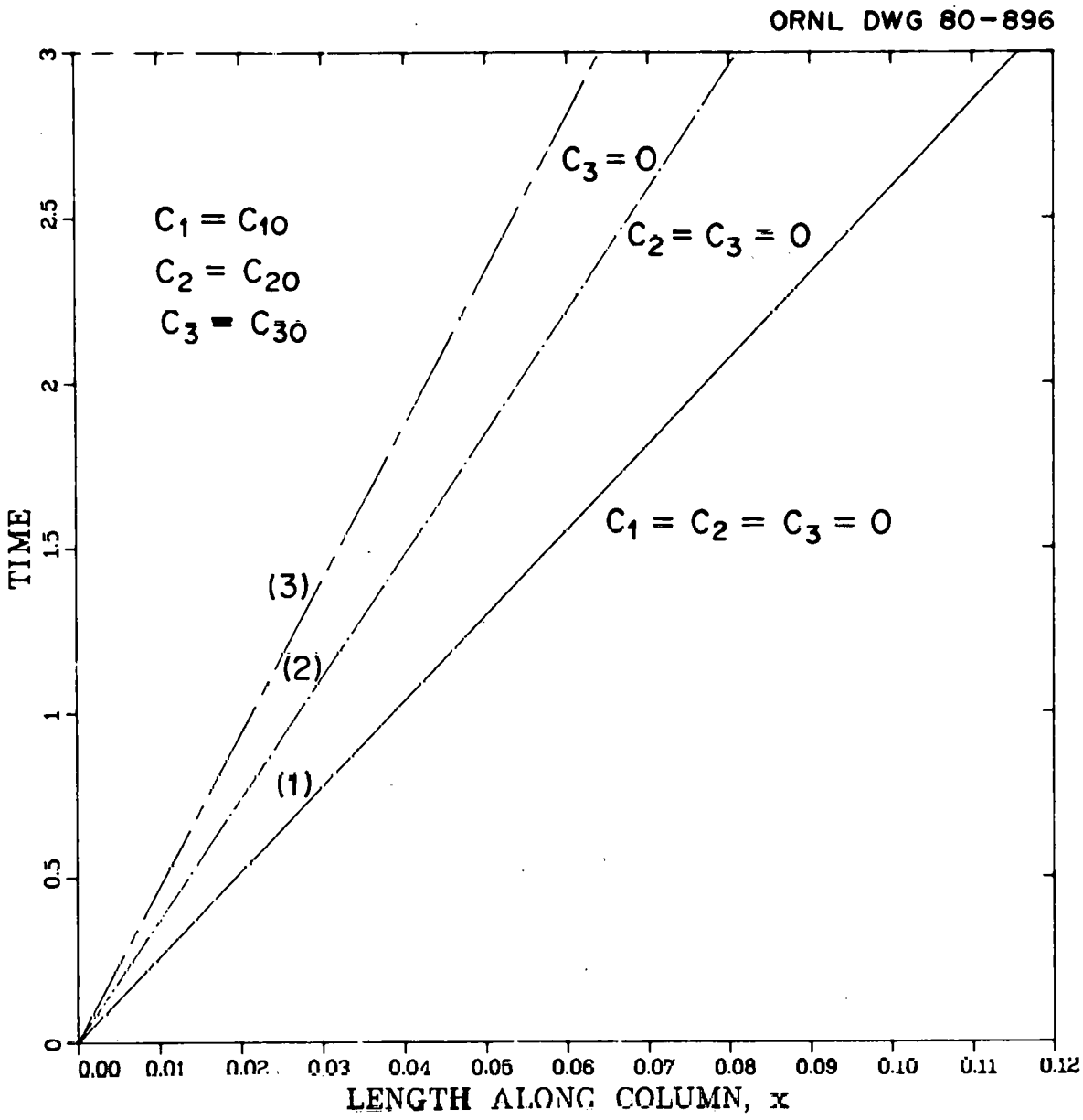

Fig. 3. Solute fronts advancing through a column in the loading of a three component mixture.

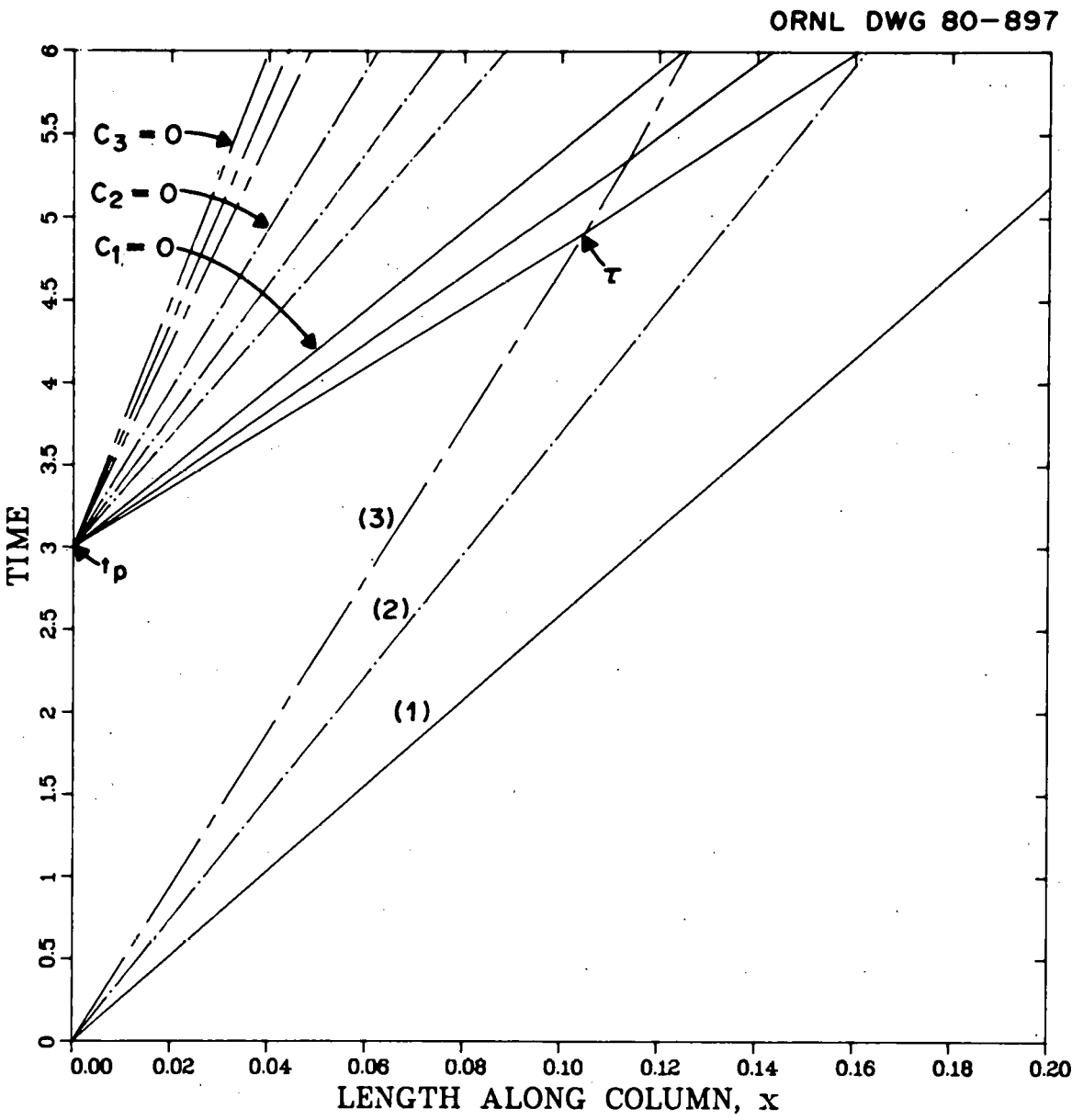

Fig. 4. Interaction of the isoconcentration lines in fan 1 with shock 3.

solute 1 is removed from the resin first). All three solutes are present along each of the isoconcentration lines in fan 1. At time, τ, fan 1 starts to overtake shock 3. This results in an interaction between the two waves. The net effect of the interaction is that shock 3 will move at a slower rate through the column (steeper slope) because there will no longer by any solute 1 competing for sites on the resin. The solvent fan 1 will also be slowed because there will be an absence of solute 3 to the right of shock 3. That is, solutes 1 and 2 will spend a greater proportion of time on the resin phase because competition from solute 3 is no longer a factor. Fan 1 will proceed down the column until it overtakes shock 2 and a similar transmissive interaction will ensue. In this case, solute 2 is depleted, leaving only solute 1 in fan 1. Again the speed at which the isoconcentration waves move through the column will be retarded due to the absence of solute 2 to the right of shock 2. This is shown in Fig. 5. When the last of fan 1 ($C_1 = 0$) has interacted with shock 2, solutes 1 and 2 will have been separated. This occurs at point A in Fig. 5. At times and bed lengths greater than those of point A, the separation distance between solutes 1 and 2 increases. Point A thus represents the minimum time and distance required to separate solutes 1 and 2.

After interaction with shock 2, fan 1 starts to interact with shock 1. Unlike the previous fan-shock interactions, the fan wave is not transmitted in this case. Instead, it is absorbed, thereby slowing the advance of shock 1. What ultimately results at long times and distances is shown on Fig. 6. The solvent front (fan 1) minimum velocity isoconcentration line (corresponding to $C_1 = 0$) moves at the same rate as the shock wave.

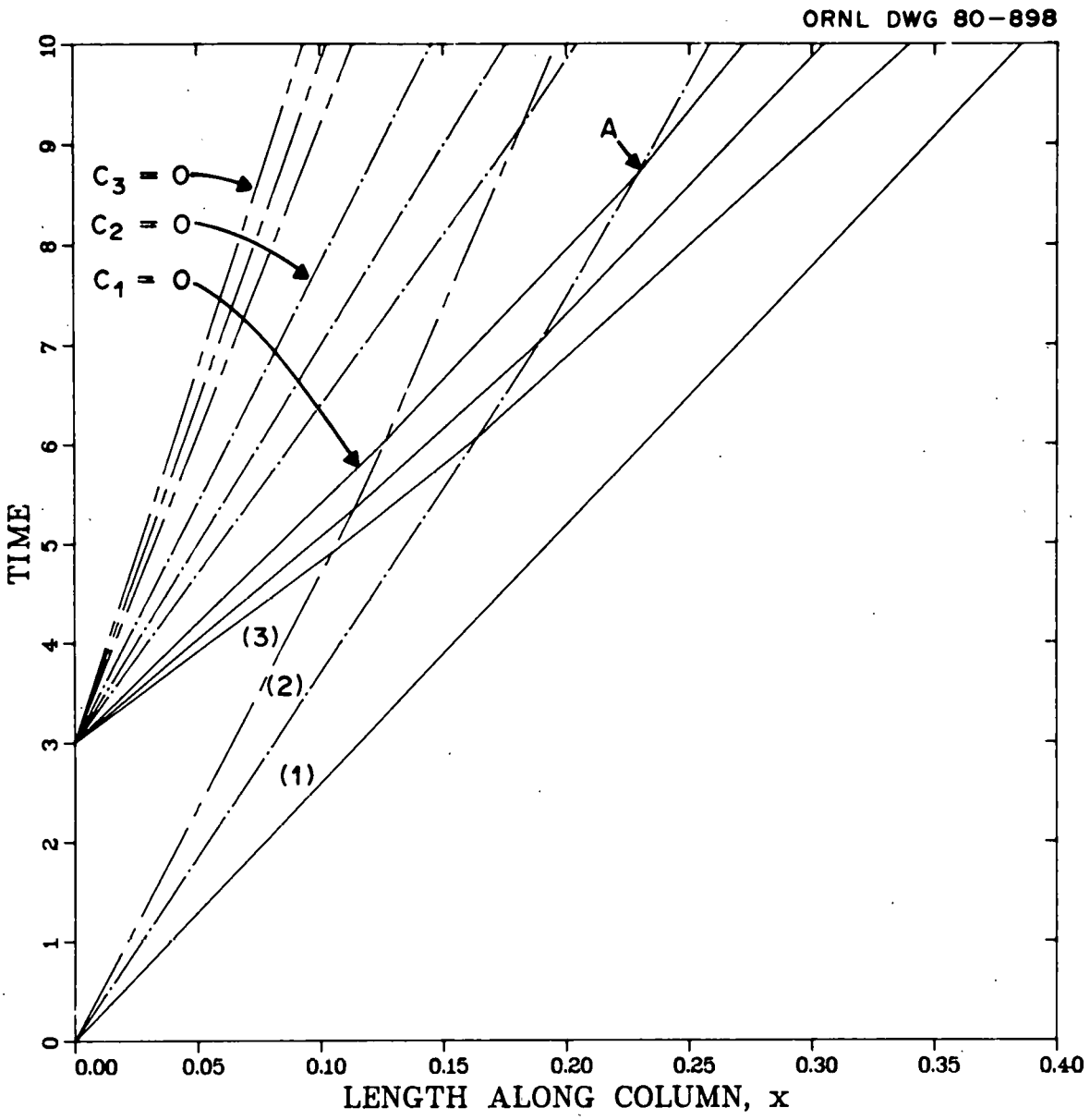

Fig. 5. Interaction of the isoconcentration lines in fan 1 with shock 2.

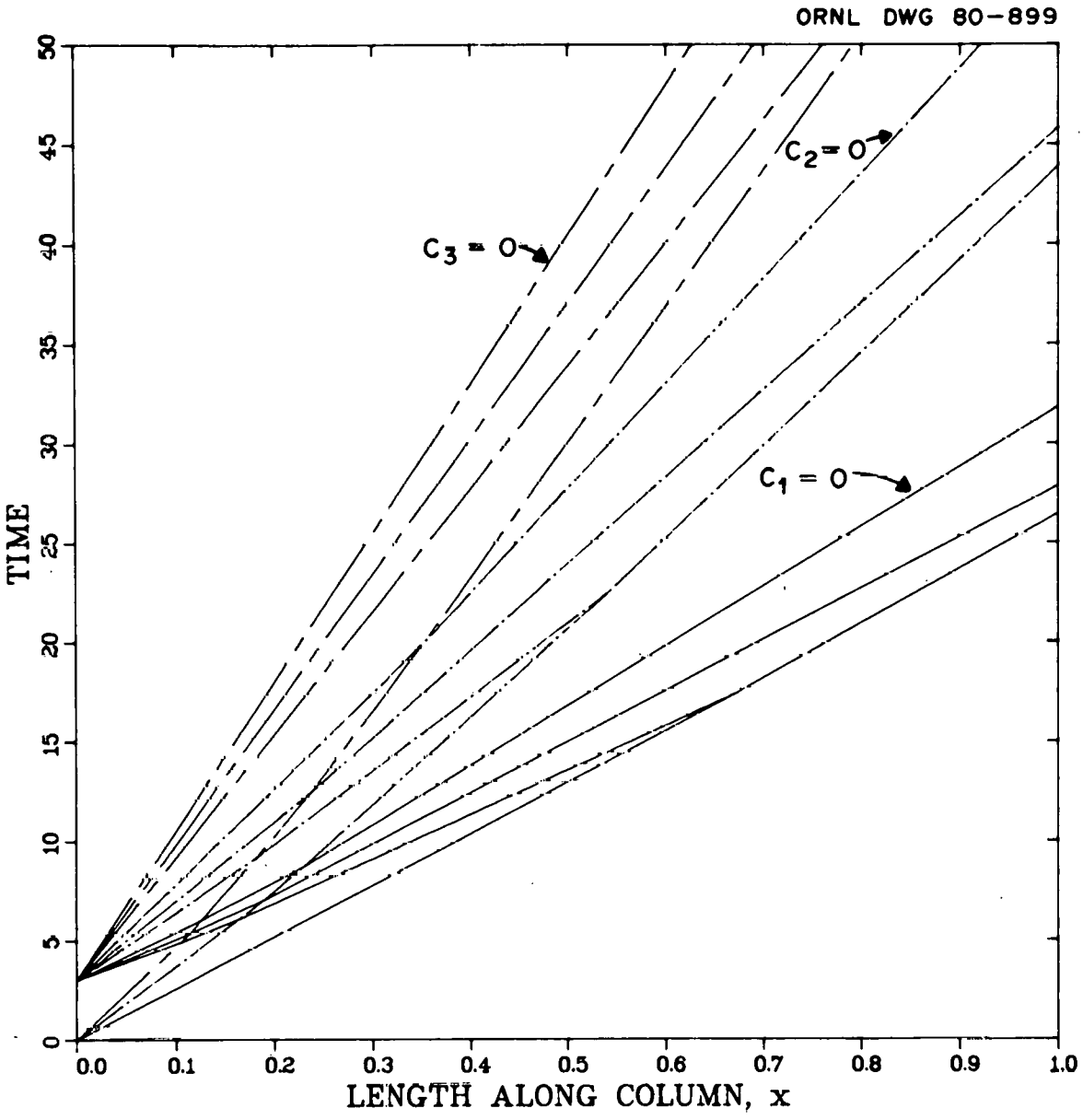

Fig. 6. Absorption of the isoconcentration lines in fan 1 with shock 1.

Thus, the two lines are parallel and separated by a constant distance at all bed lengths. This distance represents the solute 1 bandwidth.

Similar fan-shock interactions occur with the other waves. Typical final results are shown in Fig. 7 (only one fan line is shown for each fan wave). Point B depicts the time and position at which solute 2 is completely separated from solute 3. The effluent concentration profiles at any particular bed length may be determined by simply following along a vertical line through each of the shock and fan waves. Figures 8 and 9 show typical profiles for x = 0.2 and x = 1.0 respectively. At x = 0.2, there is incomplete separation between solutes 2 and 3. At x = 1.0, all three solutes have been separated.

To summarize, if one knows the inlet concentrations for each solute; the binding constants, K_i; the void volume of the column, ε; the eluent superficial velocity, v; and the total capacity of the resin, N, the effluent concentration as a function of time at any arbitrary bed length, x, can be predicted. A computer program has been written to perform the calculations and is described in detail in Appendix A.

3. CASES STUDIED

The model was tested by performing calculations based on experimental data already generated on the CAC. The experiment separated copper, nickel, and cobalt (Co-1 and Co-2) amine complexes using Dowex 50W-X8 50- to 60-μm ion exchange resin (NH_4^+ form) with 1 M $(NH_4)_2CO_3$ at pH 7.88 as the eluent.[6] The purpose of the experiments was to study the effect of variation in the feed bandwidth (t_p) on product resolution.

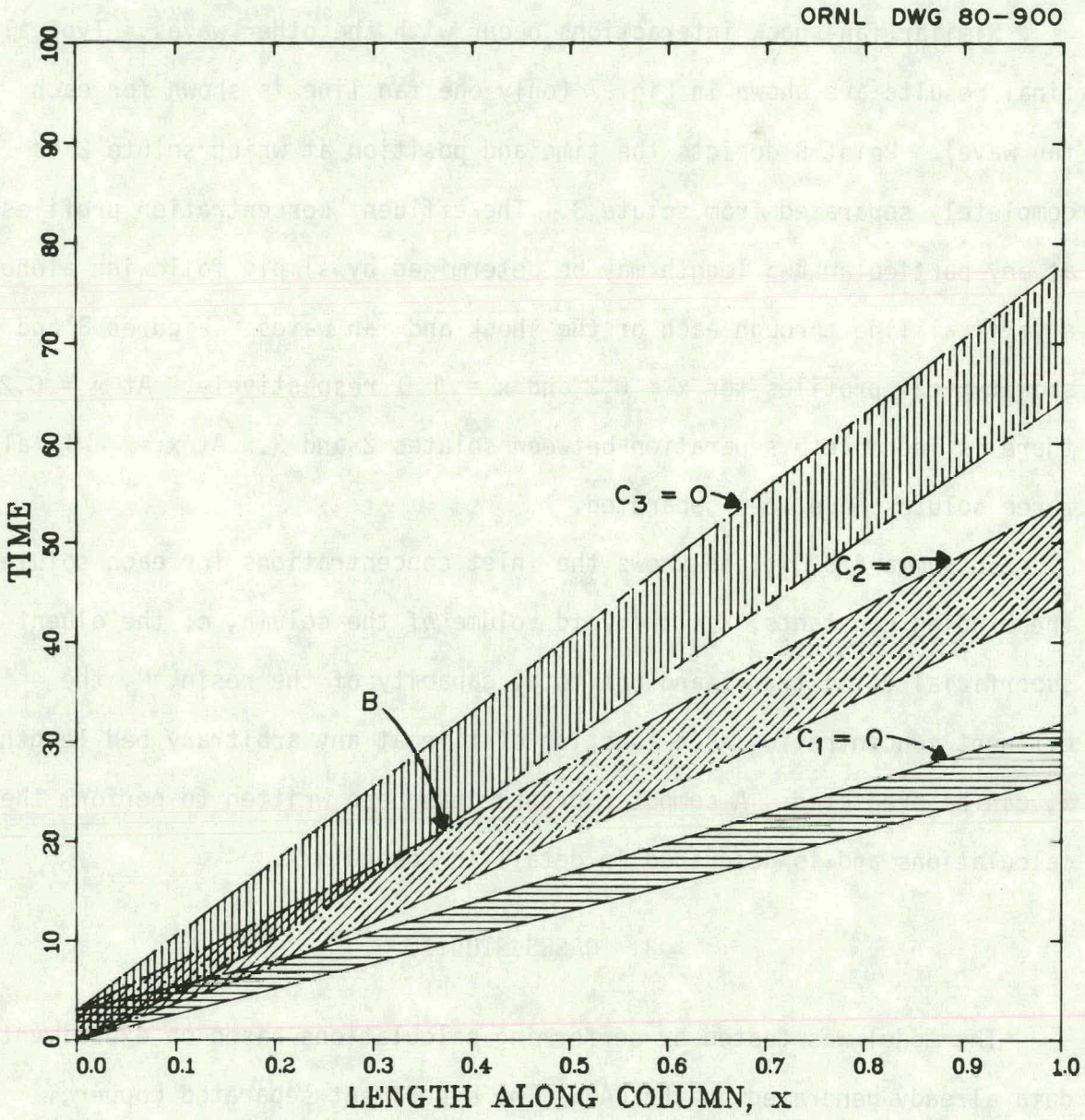

Fig. 7. Development of the solute bands along the column length.

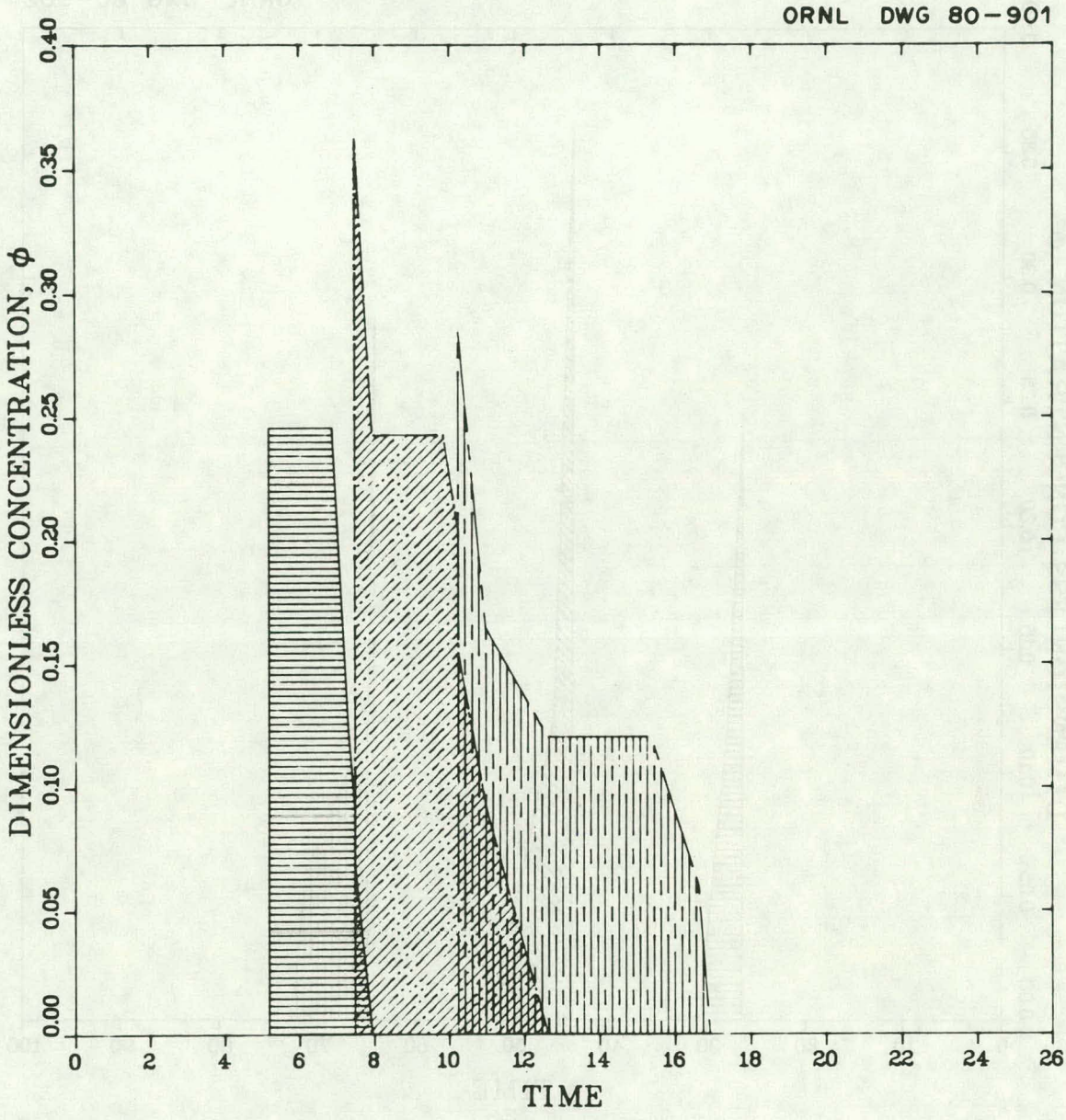

Fig. 8. Typical concentration profile at x = 0.2.

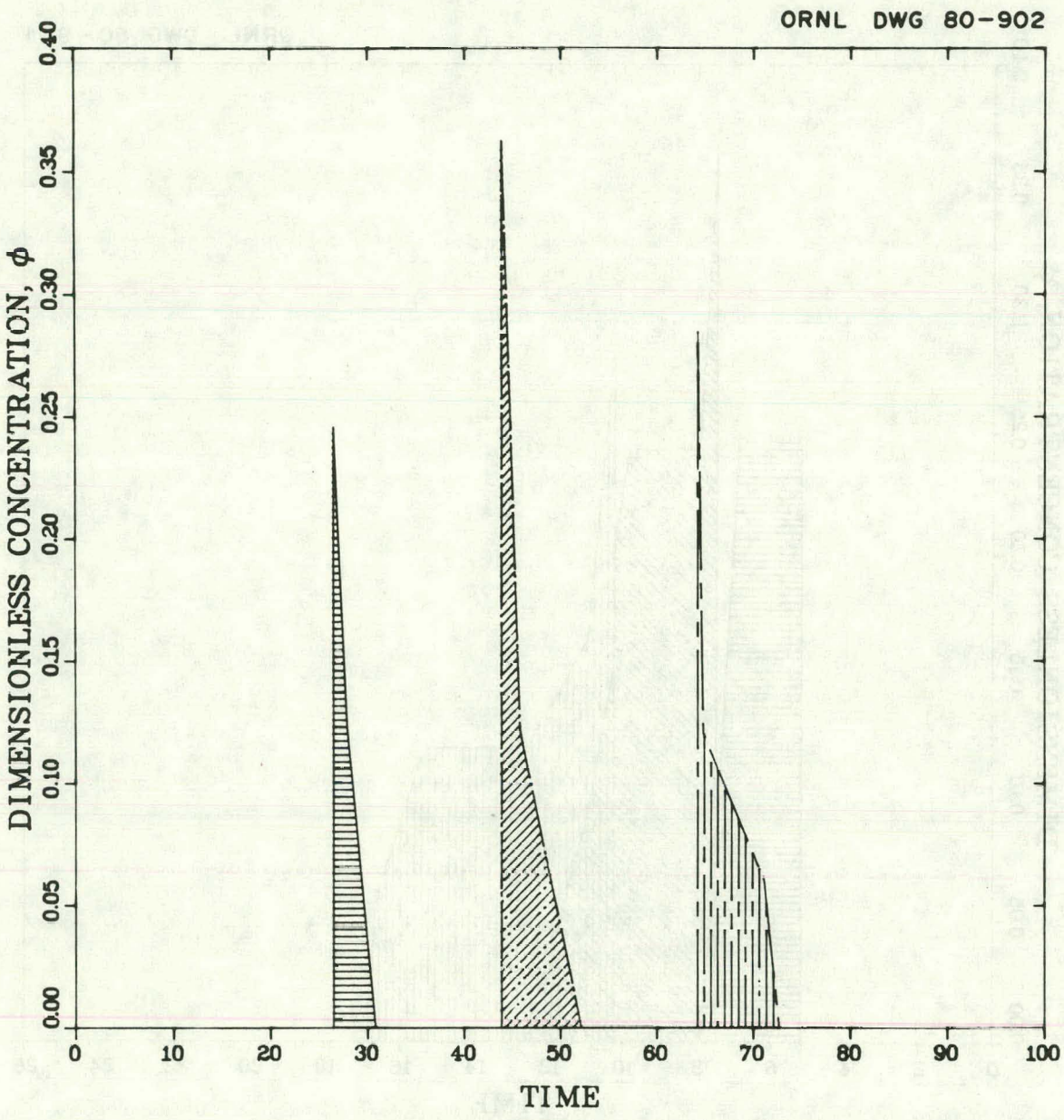

Fig. 9. Typical concentration profile at x = 1.0.

The binding constants for each of the solutes and the resin capacity used in the calculation are given in Table 2. The resin capacity used was the nominal capacity quoted by the resin manufacturer. The binding constants were determined by a trial-and-error method. Initial estimates were modified so that the results of the calculation matched those for one particular set of experimental conditions. These constants were not varied in any of the subsequent calculations. (Attempts to measure the binding constants in separate equilibrium binding experiments yielded inconsistent results, presumably due to the large errors involved in the experiments.) The algorithm used to determine the binding constants is fairly straightforward and is described in Appendix A.

Table 3 summarizes the experimental conditions used in the calculations. The feed bandwidth was varied from 5 to 38 mm. Because the bed was rotating at 62.2°/h and the diameter of the annular bed is 28.2 cm, these bandwidths correspond to pulse widths ranging from 2 to 15 min. The feed bandwidth is varied experimentally by changing the solute mixture feed rate. When the feed rate exceeds the eluent rate, the feed band spreads. Conversely, at feed rates lower than the eluent rate, the feed pulse is confined to a narrower region and undoubtedly undergoes some dilution in the process. For the cases studied here, the eluent rate was 2.53 cm/min. For feed rates less than this eluent rate, the inlet solute concentrations were assumed to be diluted in direct proportion to the ratio of feed to eluent flow rates.

Table 2. Binding isotherm data used in the model calculations

Resin capacity: N = 1.78 meq/ml resin.

Solute complex	$\underline{K}_i$ (ml solution/meq)	$\underline{K}_{app}$[a] (ml solution/ml resin)
Cu	1.18	2.10
Ni	2.18	3.88
Co-1	2.92	5.20
Co-2	7.73	13.76

[a] K_{app} is the distribution coefficient at very low concentrations:

$$B_i = \frac{NK_iC_i}{1+\sum_{j=1}^{n} K_jC_j} \approx K_{app}C_i \quad \text{if} \quad \sum_{j=1}^{n} K_jC_j << 1 \ .$$

Table 3. Experimental conditions used in the analytical model

v = 2.53 cm/min

ϵ = 0.38

L = 50 cm

Feed bandwidth = 5 to 38 mm

ω = 62.2°/h

Solute complex	C_{io}[a] [(meq/ml solution) x 10^2]	C_{io}[a] (g/liter)
Cu^{2+}	1.57	0.5
Ni^{2+}	13.63	4
$Co\text{-}1^{+}$	0.848	0.5
$Co\text{-}2^{2+}$	1.697	0.5

[a]Assuming the feed rate $\geq$ eluent rate. For the 5- and 7-mm bandwidth cases, these values were assumed to be 1.0/2.53 and 2.0/2.53 of the values shown here.

4. RESULTS

Bed concentration profiles were computed for the range of bandwidths listed in Table 3. The results predicted for a 7-mm feed bandwidth are shown in Fig. 10 on the x/L-θ plane. Solute bands for each solute in the system are represented by a pair of broken lines. The lowest band is for the copper complex, followed in order by the nickel, Co-1, and Co-2 complexes. This figure corresponds to the trajectory of the bands that would be observed during the operation of the CAC. In the calculations, L was assumed to be 50 cm, equal approximately to the overall bed length of the CAC. The effluent concentration can thus be determined by a cut at x/L = 1. This eluent profile is shown in Fig. 11 where $\phi_i (= K_i C_i)$ as a function of θ is plotted. In the case shown, the copper complex exits at 34°, the nickel complex at 55°, the Co-1 complex at 73°, and the Co-2 complex at 177°. Note that the shape of the peaks is not Gaussian. This, of course, is because dispersion effects were neglected in the calculation. Results for each of the other cases tested are shown in Figs. B.1-B.18 found in Appendix B.

Referring to the figures in Appendix B, the model predicts complete separation of all four solutes for bandwidths up to 19 mm (7.7°). With a feed bandwidth of 19 mm, the model predicts that the nickel complex will emerge slightly contaminated with Co-1. At even larger feed bandwidths, the degree of overlap between the two bands increases. For the range of bandwidths used, the model predicts complete separation of the copper and nickel complexes.

Experimentally, the nickel and Co-1 bands overlapped for feed bandwidths greater than 22 mm, in agreement with the model. However, contrary

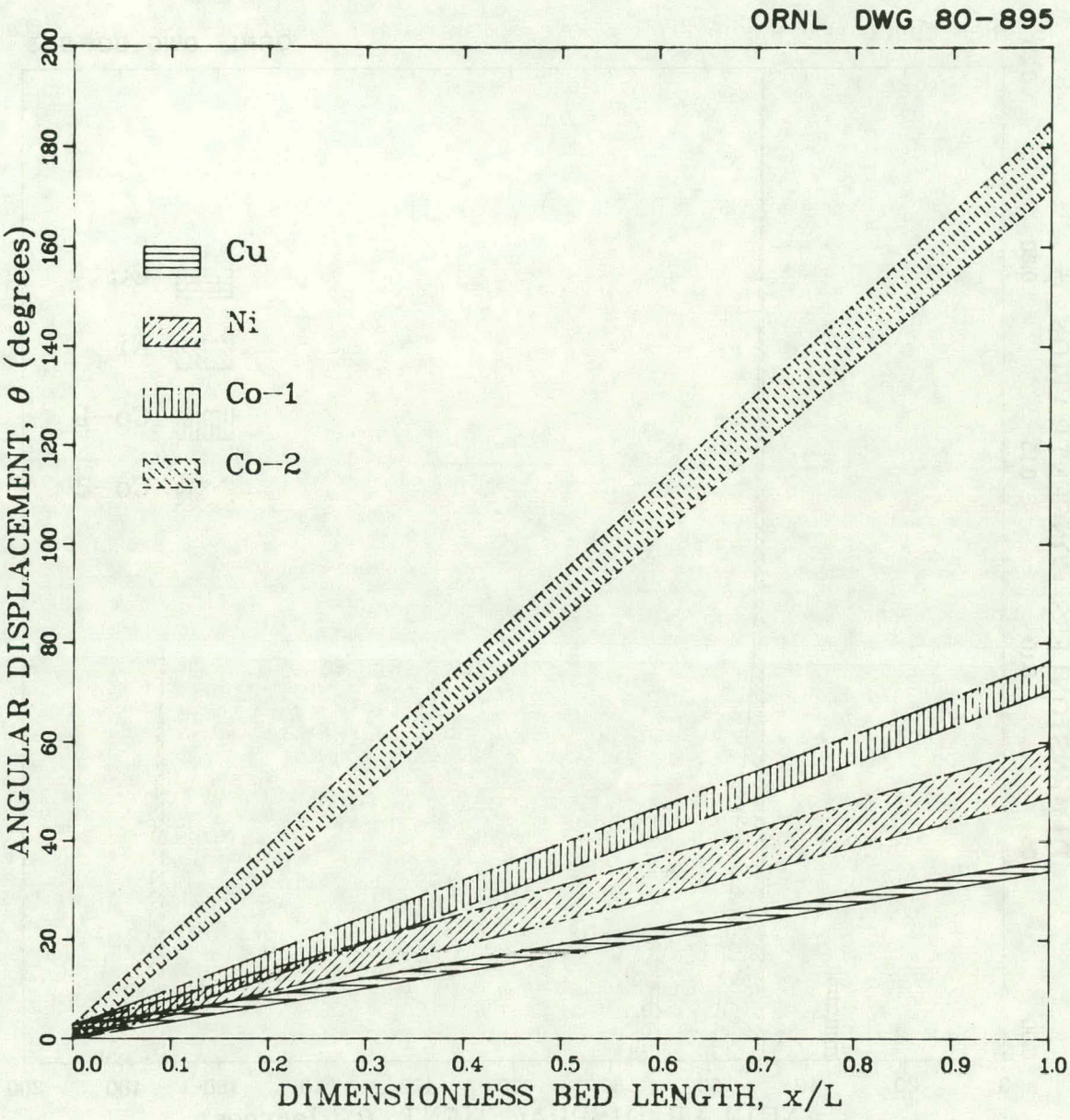

Fig. 10. Solute bands along the column length for a 7-mm feed bandwidth.

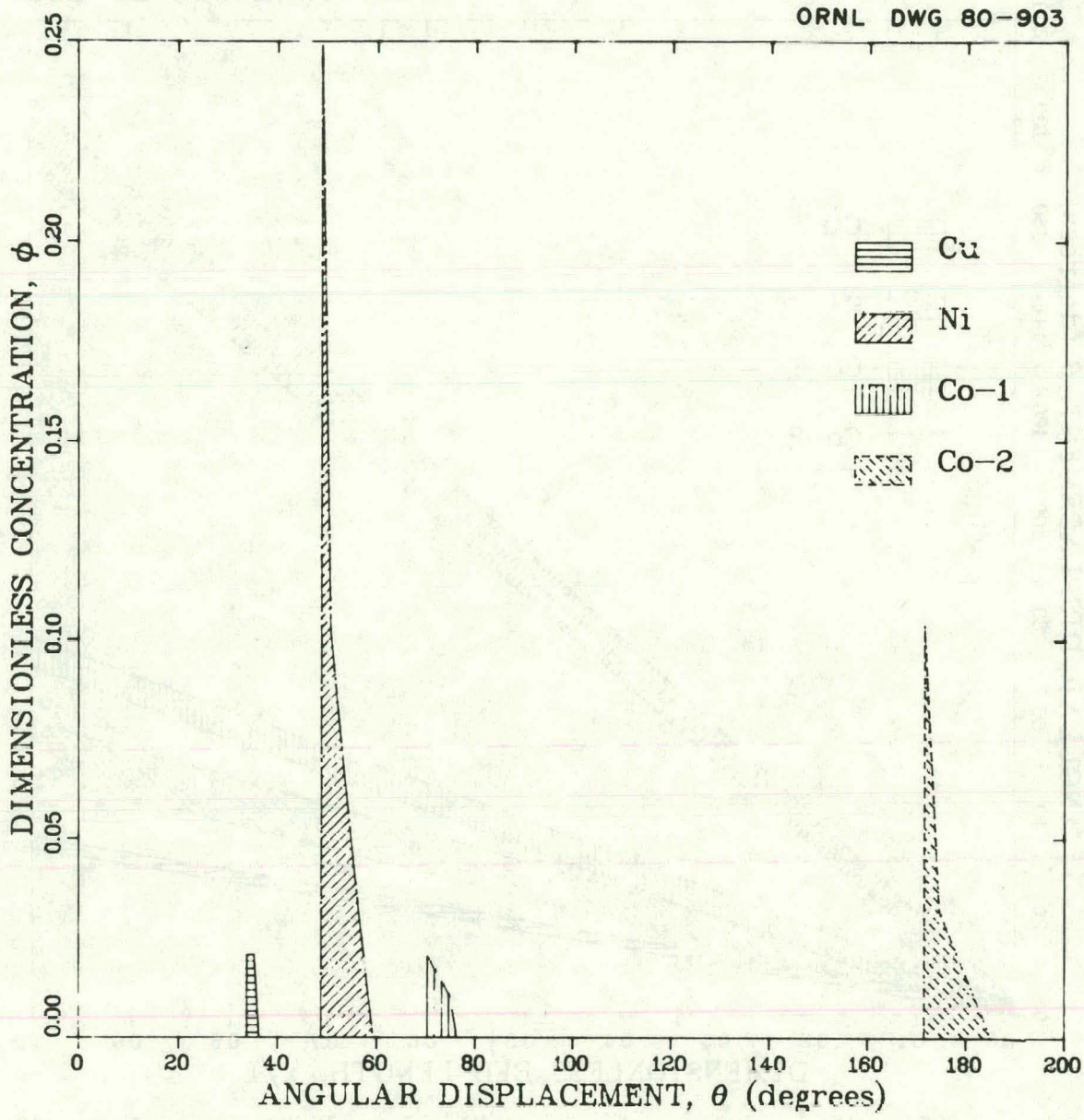

Fig. 11. Concentration profile at the column exit for a 7-mm feed bandwidth.

to predictions, the copper and nickel bands also overlapped for feed bandwidths of 19 mm and greater. This discrepancy between the model predictions and the experimental results may be explained in part by the omission of dispersion effects in the model. Also, the binding constants used in the calculation may not have been sufficiently accurate.

Although the model may not have predicted the band overlaps properly, it did a reasonably good job of estimating the position of the effluent concentration peaks. The comparison between experimentally measured and model-predicted peak positions is shown in Fig. 12. Most of the data points are scattered near the 45° line of identity. The major exception to this observation is the data for the position of the Co-2 peaks. The model generally overpredicted these peak locations, again probably due to the choice of the binding coefficient for Co-2.

The column effluent solute bandwidths predicted by the model were, in general, understandably smaller than those determined experimentally. The comparison of theory and experiment is shown in Figs. 13 and 14. In the case of copper, the model and experimental results show qualitative, but not quantitative, agreement (Fig. 13). The results obtained with nickel are somewhat surprising. Over the range of column feed bandwidths tested, the model agrees quite well with the experimental findings. Results obtained with Co-1 and Co-2 (Fig. 14) are similar to those of copper in that the model predicts the correct trend but not the correct quantitative values.

The comparison between predicted and measured peak resolution is shown in Fig. 15; peak resolution is defined in ref. 7. A value of unity means that the adjacent peaks are just touching. Values above unity infer

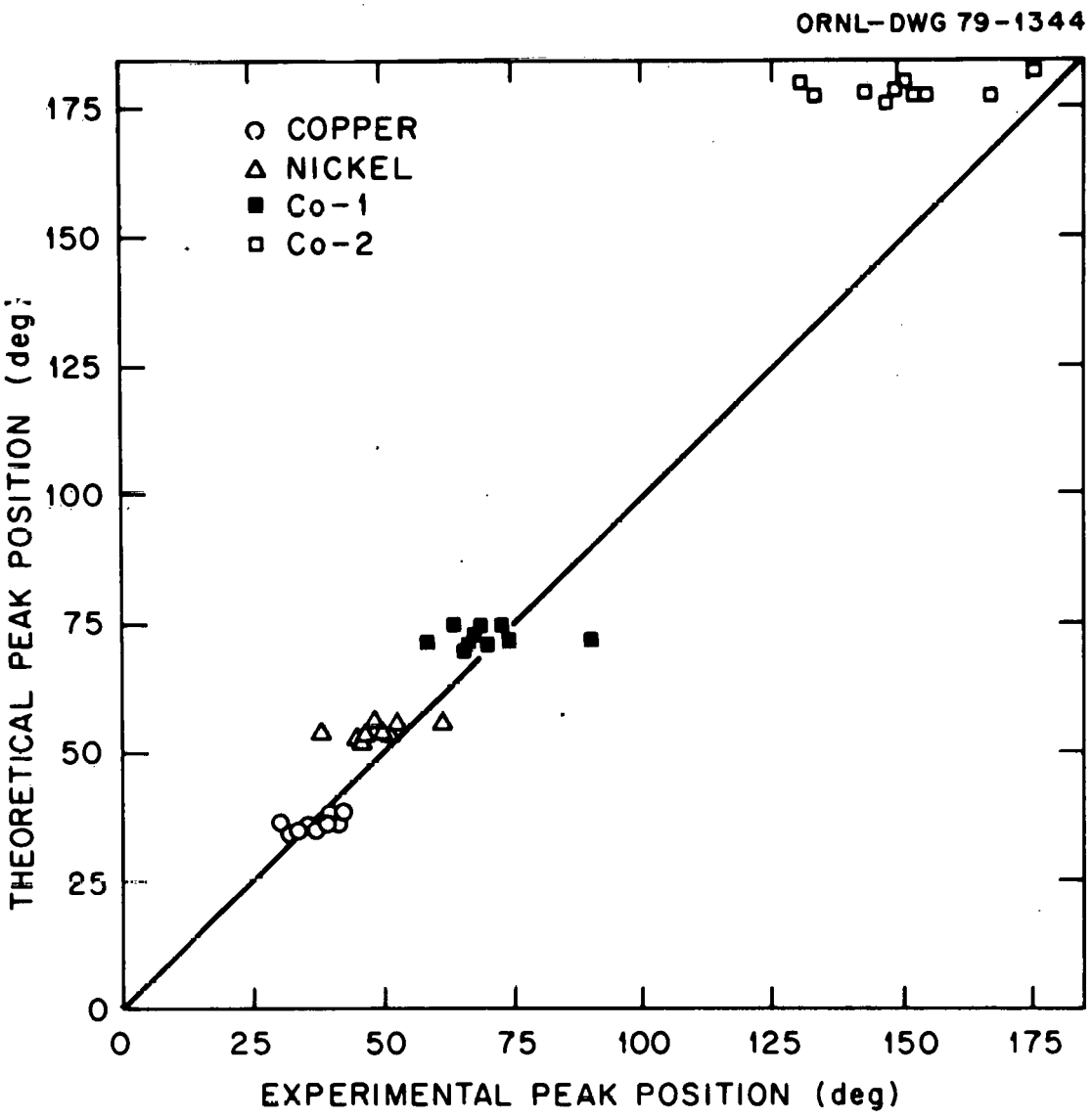

Fig. 12. Comparison of predicted and measured peak positions.

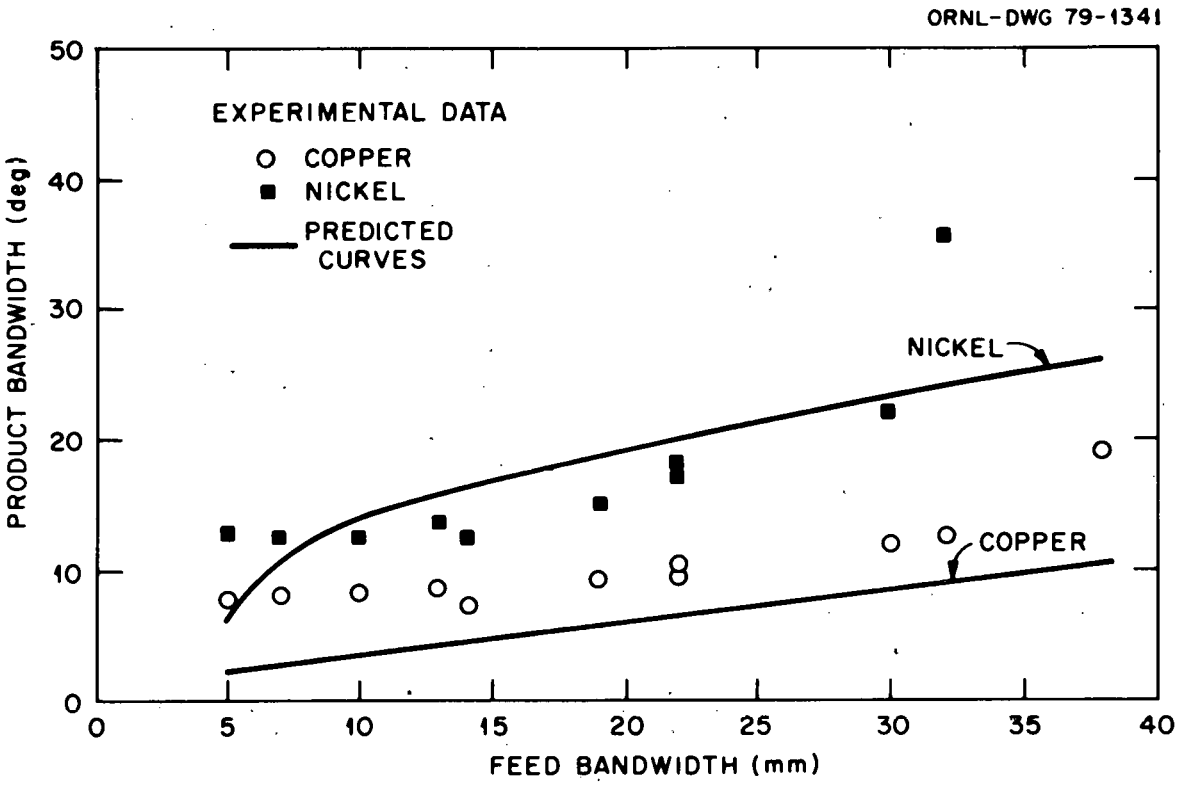

Fig. 13. Experimental and predicted product bandwidths for nickel and copper.

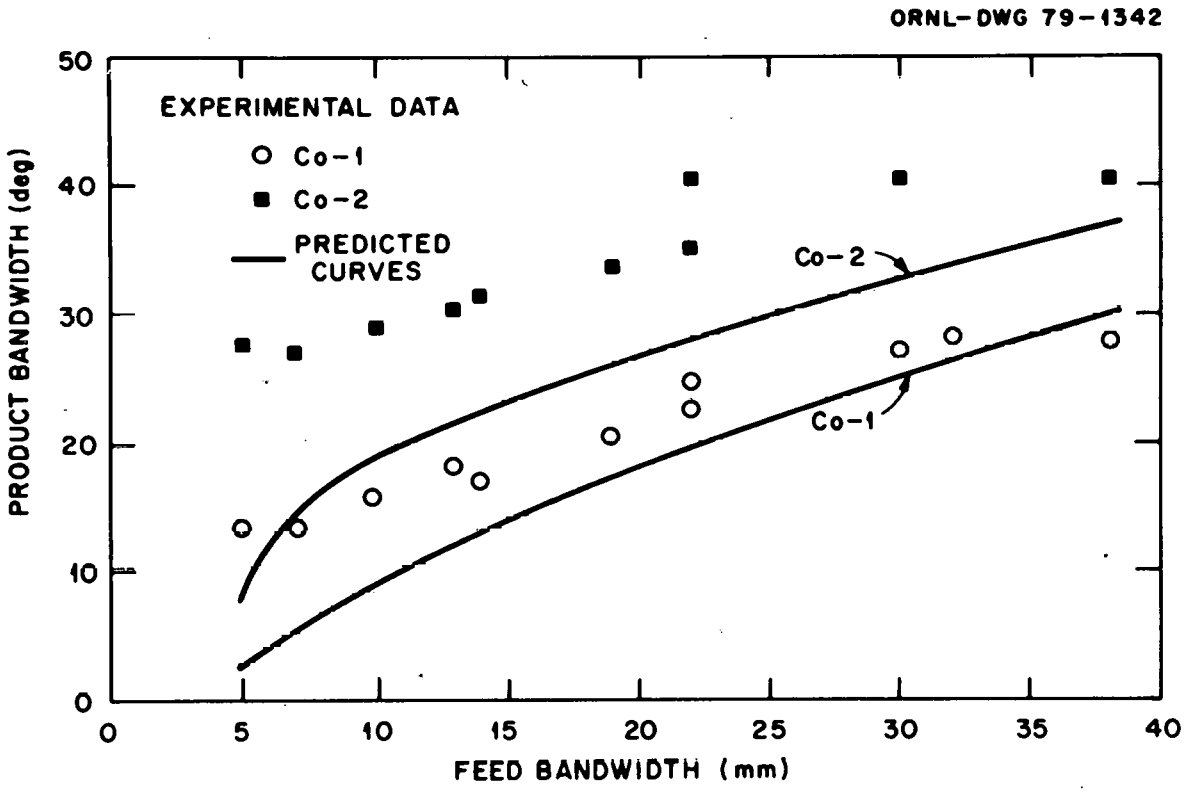

Fig. 14. Experimental and predicted product bandwidths for Co-1 and Co-2.

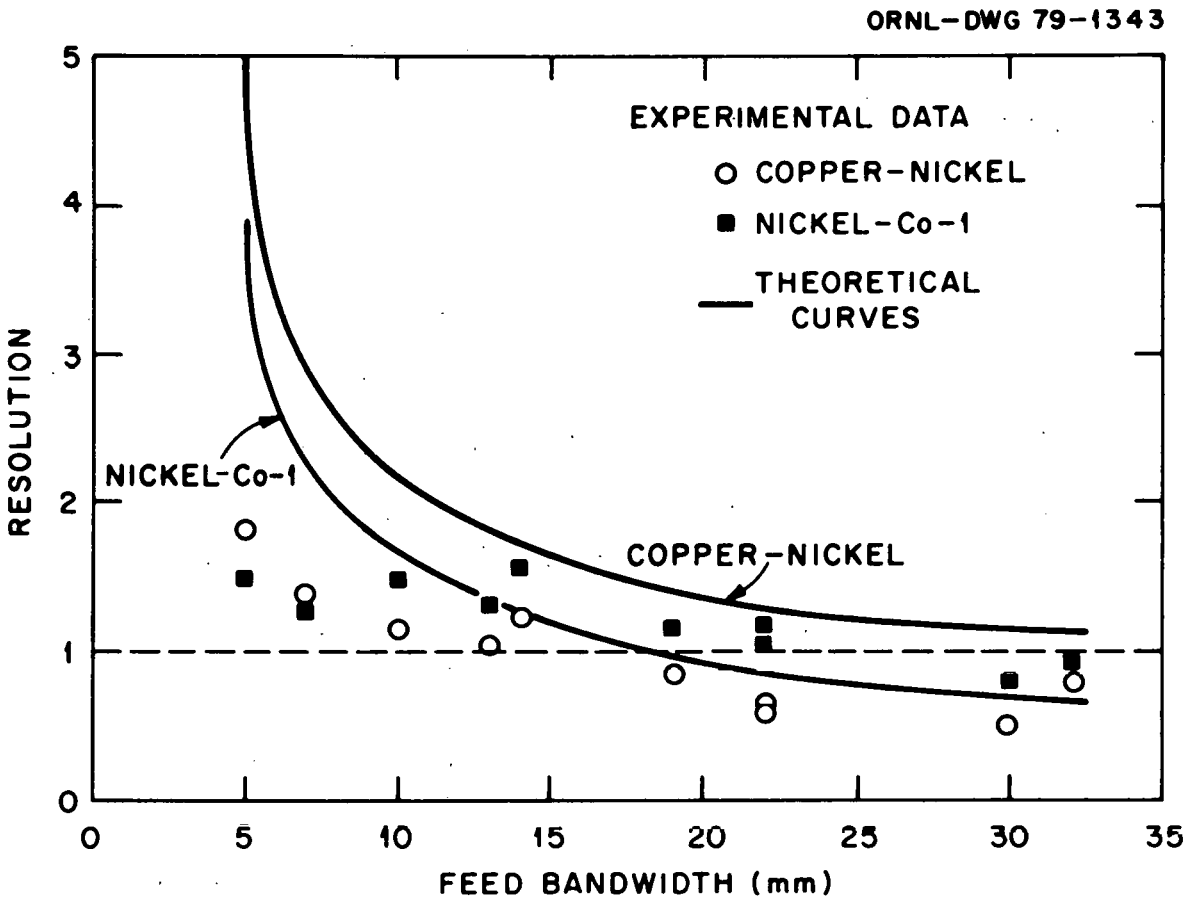

Fig. 15. Product resolution.

separation of the two solutes, and values below unity infer contamination. The model predicted separation of the copper and nickel complexes over the entire range of feed bandwidths. Experimental results showed an overlap of the two solute bands at feed bandwidths in excess of 19 mm. The agreement between the model and experimental results was better in the case of the nickel--Co-1 separation. The onset of contamination at about 22 mm was confirmed experimentally.

5. DISCUSSION

If a mathematical model is to predict the performance of the CAC accurately, it must incorporate all the effects of convection, dispersion, and nonlinear binding isotherms. The shortcoming of the model tested here is the omission of the dispersion effects. These dispersion effects are particularly important if one wishes to determine solute resolution in the column effluent. However, if only a prediction of gross behavior at different operating conditions is desired, this model may be sufficient. In models which include dispersion, it is necessary to estimate the dispersion coefficient for each solute. Since there is no reliable way to make this estimate better than within an order of magnitude, the success of these more complete models is also doubtful.

The virtues of the Rhee model are its simplicity in terms of the calculations involved and the fact that it provides a convenient framework for insight into the physical processes which occur in chromatographic separations. It also allows consideration of the interactions between solutes and the resin in multicomponent separations. For example, one could expect to predict the effect of a doubling of the inlet feed

composition of all the solutes being separated with reasonable accuracy. Another desirable feature of this approach is that the theory could be modified to account for gradient elution operations. This area might warrant future exploration in light of the successful gradient elution runs on the CAC.[6]

6. CONCLUSIONS

The multicomponent chromatographic model[2] has been compared to experimental results obtained on the CAC. The model predicts the position of the effluent solute peaks quite well under conditions of varying input feed bandwidths. It also predicts the correct trends in effluent solute resolution as the feed bandwidth is increased. Given a method for superimposing dispersion effects on the predicted output concentration profiles, one would be better able to make a quantitative prediction of band overlap and contamination. One possible use of this model would be to predict CAC performance as the solute concentrations in the feed stream were varied. More experimental data need to be generated with wide ranges in feed composition before comparisons with the model can be made. The model may be adapted for gradient elution operations, and this may prove useful in assessing the gradient elution mode in the industrial setting.

THIS PAGE

WAS INTENTIONALLY

LEFT BLANK

7. APPENDIXES

THIS PAGE

WAS INTENTIONALLY

LEFT BLANK

APPENDIX A. COMPUTER PROGRAM

All calculations were performed on a PDP-11 computer. A basic description of how to use the program follows. No attempt will be made to describe the program algorithm in detail.

1. Running the program MCHAR

Input data. Input data are read from a data file, MCHAR.DAT. The data should be in the following format:

Line 1: K_i (6F8.4 format)

Line 2: C_j^i (6F8.4 format)

Lines 3 and 4: C_{io} (4E10.4 format)

Line 5: N, ε (2F8.4 format)

Line 6: n, nic, pw, v, ω (2I2, 3F8.4 format)

where the symbols are defined in Table A.1. An example of input data is also shown in Table A.1.

In the example shown, $K_1 = 1.18$, $K_2 = 2.18$, $K_3 = 2.92$, and $K_4 = 7.73$. Note that the K_i's must be entered in ascending numerical order. Since the bed was assumed to be initially solute free, $C_j^i = 0$. The feed (entry) solute concentrations are: $C_{10} = 0.0354$, $C_{20} = 0.1533$, $C_{30} = 0.01909$, and $C_{40} = 0.03818$ meq/ml ($C_{50} = C_{60} = 0$). The resin binding capacity, N, = 1.78 meq/ml resin; $\varepsilon = 0.38$; the total number of solutes, n, = 4 (the program may handle up to six component systems); the number of isoconcentration lines in each "fan wave," nic, = 8 (8 is the maximum number possible); the feed bandwidth, pw, = 12.0 mm; the superficial eluent velocity, v, = 2.53 cm/min; and, finally, the bed rotation rate, ω, = 62.2 °/hr.

Table A.1. Program input data

Sample data file:

```
1.18, 2.18, 2.92, 7.73, 0., 0.
0., 0., 0., 0., 0., 0
3.54E-02, 1.533E-01, 1.908E-02, 3.818E-02
0.0E-00, 0.0E-00, 0.0E-00, 0.0E-00
1.78, 0.38
4, 8, 12., 2.53, 62.2
```

Notations used:

K_i - solute binding constants, ml solution/meq (line 1)

C_j^i - initial solute concentrations in ion exchange bed, meq/ml solution (line 2)

C_{io} - feed solute concentrations, meq/ml (lines 3 and 4)

N - resin binding capacity, meq/ml resin (line 5 - #1)

ε - column void fraction (line 5 - #2)

n - number of solutes (line 6 - #1)

nic - number of isoconcentration line in each "fan wave" (line 6 - #2)

pw - feed bandwidth, mm (line 6 - #3)

v - superficial eluent velocity, cm/min (line 6 - #4)

ω - column rotation rate, "/hr (line 6 - #5)

Executing the program. If MCHAR.DAT has the proper input data, only "RUN MCHAR" needs to be entered. After results are printed, the line terminal will ask if a plot is wanted (in the X-θ plane as shown in Fig. B.1). If the response is yes, the maximum values for X and θ are requested. In this case, X is the dimensionless bed length, x/L. After entering the requested value, press "return" and the plot will be made on the cathode ray terminal (CRT). A hard copy of the plot may be obtained using the "copy" key on the CRT keyboard. The line terminal will ask if another plot with different scaling is wanted; if so, it will ask for maximum values for X and θ.

Once all the desired X-θ plots have been obtained, concentration profiles may be drawn (similar to those shown on Fig. B.2) at any desired dimensionless bed length. Enter only the appropriate responses to the questions posed by the line terminal. The coordinates of the curves to be plotted are shown ahead of time on the line printer. This should aid in determining the best scaling parameters to enter.

2. Estimation of binding constants, K_i

Suppose one wishes to model a particular experimental run in which the θ_{io} (position of the peak maxima) are known. To a first approximation, the binding constants, K_i, may be estimated from:

$$\theta_v \left(1 + \left(\frac{1 - \varepsilon}{\varepsilon}\right) NK_i\right) = \theta_{io} \ , \qquad (A.1)$$

where θ_v is the angular position (in degrees) at which the pure eluent would exit (analogous to the void volume time in gel permeation chromatography).

$$\theta_v = \frac{\varepsilon\omega x}{v} \quad . \tag{A.2}$$

These relationships are exact if the competitive binding effects among the solutes are minimal. The program-predicted θ_{io} will differ from the experimental values to the extent that competitive binding is important. A second guess of the K_i may be made based on the following:

$$\frac{K_{i\text{-program}}}{\theta_{i\text{-program}} - \theta_v} = \frac{K_{i\text{-new}}}{\theta_{i\text{-expt}} - \theta_v} \quad . \tag{A.3}$$

The $K_{i\text{-new}}$ which is calculated will usually result in $\theta_{i\text{-program}}$, which matches the experimental values quite closely.

3. Program components

The program FORTRAN code consists of a MAIN section (called MCHAR for method of characteristics) and subroutines. MCHAR calls all the necessary subroutines and function subprograms. A listing of the various subroutines and program organization is shown in Fig. A.1.

4. Program listing

The detailed FORTRAN code is listed on the following pages.

ORNL DWG 80-904

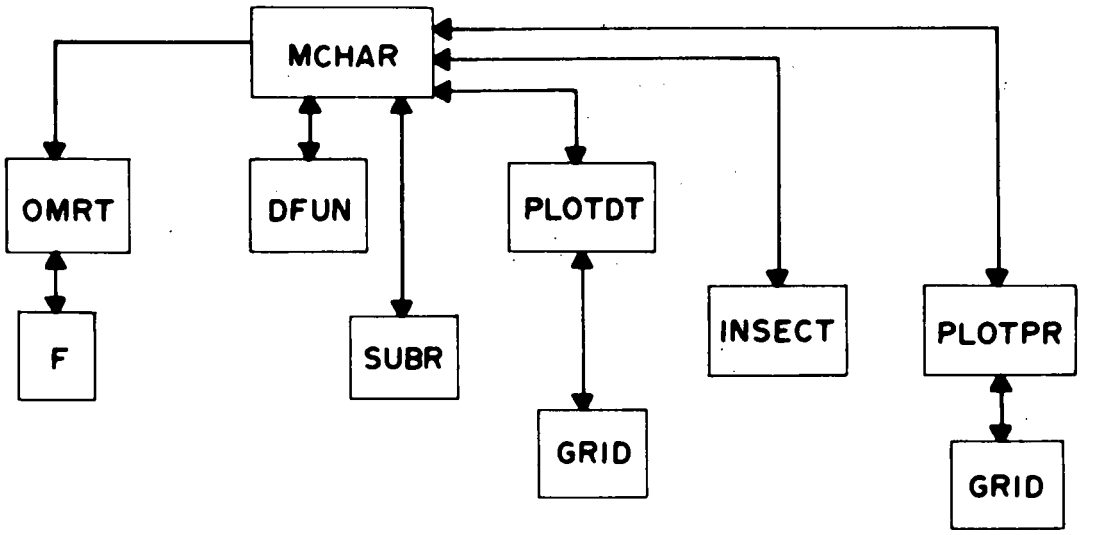

Functions of subprograms

1. MCHAR - main driving program; calculates initial slopes of shock waves and fan waves; calculates initial isoconcentrations associated with all waves.

2. OMRT,F - finds ω_i's as defined in ref. 2.

3. DFUN - calculates $1 + \sum_{i=1}^{n} K_i C_i$.

4. SUBR - determines intersection coordinates and new isoconcentrations associated with shock and fan waves.

5. PLOTDT - plots X-θ figures on CRT.

6. GRID - supplies grid for plots.

7. INSECT - determines the coordinates of all shock and fan waves at a particular bed length.

8. PLOTPR - plots concentration profiles.

Fig. A.1. Organization of program.

```
      REAL*4 K(6),N,NM(6,6),LA(6),NE(6),NI(6)
      LOGICAL*1 XDATE(9),XTIME(8)
      DIMENSION CI(6),CE(6),PHII(6),PHIE(6),D(6),PHIC(6,6),SSH(6),
     1DD(6,8),XJ(6,6),PHI(6,6,6,8),XS(6,6,8),TAU(6,6,8),WI(6),
     1 WE(6), SCW(6,8),DS(6),PHICS(6,6),NMS(6,6),ETA(8),TAUA(6),
     2 DEG(6,6,8), DEGA(6),TI(72),PHICON(72,6),DEE(72)
      COMMON TY,SSH,SCW,TAU,DD,D,WE,WI,EPS,PHI,N,K,DI,DE,TAUA
     1 ,V,ROT
      COMMON /BLK2/ XDATE,XTIME
      COMMON /BLK3/  XISO,PHICS,DEE,PHICON,ICNT
      COMMON /BLK4/ DEG,XS,M,NIC,TYD,DEGA
      CALL ASSIGN(2,'MCHAR.DAT',9)
      CALL ASSIGN(1,'TT7:')
      READ(2,1000) K
      READ(2,1000) CI
      READ(2,1050) CE
      READ(2,1000) N,EPS
      READ(2,1100) M,NIC,PW,V,ROT
      CALL DATE(XDATE)
      CALL TIME(XTIME)
      WRITE(6,1110) XDATE,XTIME,K,CI,CE
      WRITE(6,1120) N,PW,V,ROT
      TY=.470763*PW*V/ROT
      DO 100 J=1,M
      PHII(J)=K(J)*CI(J)
      PHIE(J)=K(J)*CE(J)
100   CONTINUE
      DE=DFUN(PHIE)
      DI=DFUN(PHII)
      DO 200 J=1,M
      NE(J)=N*PHIE(J)/DE
      NI(J)=N*PHII(J)/DI
200   CONTINUE
      CALL OMRT(N,K,NI,M,WI,IER)
      GO TO (210,2000), IER
210   WRITE(6,1130) WI
      CALL OMRT(N,K,NE,M,WE,IER)
      GO TO (220,2100), IER
220   WRITE(6,1140) WE
      DO 500 IM=1,M
      DO 400 KK=1,M
      PROD=PHIC(IM)
      DK=DE
      DO 300 J=1,KK
      PROD=PROD*(1.-N*K(IM)/WI(J))/(1.-N*K(IM)/WE(J))
      IF (IM .GT. 1) GO TO 300
      DK=DK*WE(J)/WI(J)
300   CONTINUE
      IF (IM .GT. 1) GO TO 320
      D(KK)=DK
320   PHIC(IM,KK)=PROD
      NM(IM,KK)=N*PHIC(IM,KK)/D(KK)
400   CONTINUE
500   CONTINUE
```

```
      WRITE(6,1150)
      DO 600 KK=1,M
      WRITE(6,1200) KK,(PHIC(IM,KK),IM=1,M)
600   CONTINUE
      DO 645 IM=1,M
      DO 640 KK=1,M
      PROD=PHIE(IM)
      DK=DE
      DO 630 J=KK+1,M
      IF (J .GT. M) GO TO 638
      PROD=PROD*(1.-N*K(IM)/WI(J))/(1.-N*K(IM)/WE(J))
      DK=DK*WE(J)/WI(J)
630   CONTINUE
      IF (IM .GT. 1) GO TO 635
      DS(KK+1)=DK
635   PHICS(IM,KK)=PROD
      NMS(IM,KK)=N*PHICS(IM,KK)/DS(KK+1)
      GO TO 640
638   DS(1)=DI
      PHICS(IM,KK)=PHIE(IM)
      NMS(IM,KK)=NE(IM)
640   CONTINUE
645   CONTINUE
      DO 650 IM=1,M
      SSH(IM)=EPS+(1.-EPS)*WE(IM)/DS(IM)
650   CONTINUE
      DELD=D(1)-DE
      DO 700 KK=1,M
      LA(KK)=WI(KK)*D(KK)
      DO 670 L=1,NIC
      XL=NIC-L
      DD(KK,L)=D(KK)-XL*DELD/(NIC-1)
      SCW(KK,L)=EPS+(1.-EPS)*LA(KK)/DD(KK,L)**2
      DO 660 IM=1,M
      IF (IM .NE. KK) GO TO 655
      IF ( KK .EQ. 1) GO TO 652
      DOLD=D(KK-1)
      PHIOLD=PHIC(IM,KK-1)
651   XJ(IM,KK)=PHIOLD/(DOLD-D(KK))
      GO TO 657
652   DOLD=DE
      PHIOLD=PHIE(IM)
      GO TO 651
655   XJ(IM,KK)=K(IM)*NM(IM,KK)/(N*K(IM)-WI(KK))
657   PHI(M,IM,KK,L)=PHIC(IM,KK)+XJ(IM,KK)*(DD(KK,L)-D(KK))
660   CONTINUE
670   CONTINUE
      DELD=D(KK+1)-D(KK)
700   CONTINUE
      WRITE(6,1240)
      WRITE(6,1250) SSH
      WRITE(6,1290)
      DO 710 KK=1,M
      WRITE(6,1300) KK,(SCW(KK,LL),LL=1,NIC)
```

```
710   CONTINUE
      WRITE(6,1340)
      DO 720 KK=1,M
      WRITE(6,1300) KK,(DD(KK,L),L=1,NIC)
720   CONTINUE
      WRITE(6,1390)
      DO 750 KK=1,M
      DO 740 L=1,NIC
      WRITE(6,1400) KK,L,(PHI(M,IM,KK,L),IM=1,M)
740   CONTINUE
750   CONTINUE
      WRITE(6,1430)
      DO 770 KK=1,M
      WRITE(6,1440) KK,(PHICS(IM,KK),IM=1,M)
770   CONTINUE
      CALL SUBR
      TYD=ROT*TY*50./(V*60.)
      CALL PLOTDT
780   TYPE 2400
      ACCEPT 2500,IA
      IF (IA .EQ. 0) CALL FINITT(0,700)
C
C         FIND INTERSECTIONS WITH SHOCK WAVES
C
      CALL INSECT
      CALL PLOTPR(M)
      TYPE 2600
      ACCEPT 2700,IA
      IF (IA .NE. 0) GO TO 780
      CALL FINITT(0,700)
1000  FORMAT(6F8.4)
1050  FORMAT(4E16.4)
1100  FORMAT(2I2,3F8.4)
1110  FORMAT('1',//T10,9A1,3X,8A1,//T10,'INPUT DATA',/T10,10('*'),///
     1T20,'K''S:',/T20,3('*'),//T20,6F10.4,//T20,'CI''S:',/T20,
     24('*'),//T20,6F10.4,///T20,'CE''S:',/T20,4('*'),//T20,6F10.4)
1120  FORMAT(///T20,'N=',F5.2,' MEQUIV/ML',/T20,'PULSE WIDTH=',
     1 F4.1,' MM',/T20,'SUPERFICIAL VELOCITY=',F5.2,' CM/MIN',/T20,
     2 'ROTATION RATE=',F4.0,' DEGREES/HR')
1130  FORMAT(///T20,'OMEGA-ENTRY''S:',/T20,13('*'),//T20,6F10.4)
1140  FORMAT(//T20,'OMEGA-INITIAL''S:',/T20,16('*'),//T20,6F10.4)
1150  FORMAT('1',//T10,'CONSTANT CONCENTRATIONS',/T10,23('*'),//T20,
     1 'WAVE NO.',T40,'PHI',/T30,80('*'),/)
1200  FORMAT(T23,I2,T30,6E13.3)
1240  FORMAT(////,T10,'SLOPES OF SHOCK WAVES=',/)
1250  FORMAT(T20,6E13.3)
1290  FORMAT(////,T10,'INITIAL SLOPES OF C-WAVES=',//T20,'WAVE NO.',
     1 T30,'L=1',T43,'L=2',T56,'L=3',T69,'L=4',T82,'L=5',/)
1300  FORMAT(T23,I2,T28,8E11.3)
1340  FORMAT(////,T10,'VALUES FOR D=',/)
1390  FORMAT(////T10,'ISO-CONCENTRATIONS (INITIAL)=',//T20,'WAVE NO.',
     1 T30,'L',T40,'M',//)
1400  FORMAT(T23,I2,T30,I1,T38,6E13.3)
1430  FORMAT(////T10,'ISOCONCENTRATIONS ASSOCIATED WITH SHOCK WAVES',
```

```
     1 /T20,'WAVE NO.',T33,'M',/)
1440  FORMAT(T23,I2,T29,6E13.3)
2000  WRITE(6,2200)
      STOP
2100  WRITE(6,2300)
      STOP
2200  FORMAT('1',//T10,'***ERROR***-NO ROOT COULD BE FOUND FOR ''WI''.
     1  CHECK INPUT DATA.')
2300  FORMAT('1',/T10,'***ERROR***NO ROOT COULD BE FOUND FOR ''WE''.
     2  CHECK INPUT DATA.')
2400  FORMAT(' DO YOU WANT ANY PLOTS OF CONCENTRATION PROFILES?
     1(0=NO; 1=YES):',$)
2500  FORMAT(I2)
2600  FORMAT(' DO YOU WANT ANOTHER PLOT OF CONCENTRATION PROFILES
     1 AT A LARGER BED LENGTH? (0=NO; 1=YES):',$)
2700  FORMAT(I2)
      END
```

```
      SUBROUTINE OMRT(N,K,NI,M,WI,IER)
      REAL*4 N,K(6),NI(6)
      DIMENSION WI(6)
      DO 700 J=1,M
      IF (NI(J) .NE. 0) GO TO 50
      WI(J)=N*K(J)
      GO TO 700
50    IF (J .EQ. 1) XL=.0001
      IF (J .NE. 1) XL=N*K(J-1)+.0001
      XR=N*K(J)-.0001
      FL=F(XL,K,NI,N,M)
      FR=F(XR,K,NI,N,M)
      IF(FL/FR .GT. 0.) GO TO 800
      IF (FL .LT. 0.) GO TO 100
      XPOS=XL
      XNEG=XR
      GO TO 300
100   XNEG=XL
      XPOS=XR
300   X=.5*(XPOS+XNEG)
      DO 400 I=1,50
      FX=F(X,K,NI,N,M)
      IF (ABS(FX) .LT. .001) GO TO 600
      IF (FX .LT. 0.) GO TO 320
      XPOS=X
      GO TO 340
320   XNEG=X
340   X=.5*(XPOS+XNEG)
400   CONTINUE
      WRITE(6,1000) J
      IER=2
      RETURN
600   WI(J)=X
700   CONTINUE
      IER=1
      RETURN
800   WRITE(6,1100)
      IER=2
      RETURN
1000  FORMAT('1',/T10,'***ERROR***-NO ROOT COULD BE FOUND FOR J=',I2,
     1' IN OMRT.')
1100  FORMAT('1',/T10,'***ERROR***-INITIAL ESTIMATES DID NOT BRACKET
     1 THE SOLUTION IN OMRT.')
      END
```

```
      FUNCTION F(X,K,NI,N,M)
      REAL*4 K(6),NI(6),N
      SUM=0.
      DO 100 I=1,M
      SUM=SUM+K(I)*NI(I)/(N*K(I)-X)
100   CONTINUE
      F=1.-SUM
      RETURN
      END
```

```
      FUNCTION DFUN(PHI)
      DIMENSION PHI(6)
      DFUN=0.
      DO 100 I=1,6
      DFUN=DFUN+PHI(I)
100   CONTINUE
      DFUN=DFUN+1.0
      RETURN
      END
```

```
      SUBROUTINE SUBR
      REAL*4 K(6),N,NM(6,6),LA(6),NE(6),NI(6)
      LOGICAL*1 XDATE(9),XTIME(8)
      DIMENSION CI(6),CE(6),PHII(6),PHIE(6),D(6),PHIC(6,6),SSH(6),
     1DD(6,8),XJ(6,6),PHI(6,6,6,8),XS(6,6,8),TAU(6,6,8),WI(6),
     1 WE(6), SCW(6,8),DS(6),PHICS(6,6),NMX(6,6),ETA(8),TAUA(6),
     2 DEG(6,6,8), DEGA(6)
      COMMON TY,SSH,SCW,TAU,DD,D,WE,WI,EPS,PHI,N,K,DI,DE,TAUA
     1 ,V,ROT
      COMMON /BLK2/ XDATE,XTIME
      COMMON /BLK4/ DEG,XS,M,NIC,TYD,DEGA
      TI=0.
      XI=0.
      DO 950 KK=1,M
      IF (KK .NE. 1) TI=TAU(M,KK-1,NIC)
      IF (KK .NE. 1) XI=XS(M,KK-1,NIC)
      XS(M,KK,1)=(TY-TI+SSH(M)*XI)/(SSH(M)-SCW(KK,1))
      TAU(M,KK,1)=SCW(KK,1)*XS(M,KK,1)+TY
      DIN=DD(KK,1)
      DO 900 IM=M,1,-1
      OMNEW=WI(IM)
      OMOLD=WE(IM)
      IF(KK .LT. IM) WRITE(6,1450) IM
      DO 850 L=1,NIC
      IF (IM .NE. M) GO TO 833
      IF (KK .EQ. M) GO TO 833
      IF (L .EQ. NIC) GO TO 820
      XS(IM,KK,L+1)=XS(IM,KK,1)*(DD(KK,L+1)*(DIN-DD(KK,NIC)*WI(KK)/
     1OMNEW)/(DIN*(DD(KK,L+1)-DD(KK,NIC)*WI(KK)/OMNEW)))**2
      TAU(IM,KK,L+1)=SCW(KK,L+1)*XS(IM,KK,L+1)+TY
820   IF (IM .GT. KK) SCW(KK,L)=EPS+(1.-EPS)*(OMNEW/OMOLD)*WI(KK)*
     1 DD(KK,NIC)/ (DD(KK,L))**2
      SSH(IM)=EPS+(1.-EPS)*OMNEW/DD(KK,NIC)
      SUM=0.
      DO 830 I=1,M
      IF (IM .EQ. 1) GO TO 850
      IF (I .EQ. IM) GO TO 822
      PHI(IM-1,I,KK,L)=PHI(IM,I,KK,L)*(1.-N*K(I)/OMNEW)/
     1 (1.-N*K(I)/OMOLD)
      GO TO 824
822   PHI(IM-1,I,KK,L)=0.
824   SUM=SUM+PHI(IM-1,I,KK,L)
830   CONTINUE
      IF (KK .LT. IM) WRITE(6,1500) KK,L,(PHI(IM-1,I,KK,L),I=1,M)
      DD(KK,L)=SUM+1.
      GO TO 850
833   IF (IM .NE. KK) GO TO 846
      IF (IM .NE. M) GO TO 834
      IF (L .GT. 1) GO TO 8331
      XS(IM,KK,1)=(TY-TAU(IM,KK-1,NIC)+SSH(IM)*XS(IM,KK-1,NIC))/
     1 (SSH(IM)-SCW(KK,1))
      TAU(IM,KK,1)=SCW(KK,1)*XS(IM,KK,1)+TY
      GO TO 820
8331  DOLD=DD(KK-1,NIC)
```

```
      DNEW=D(KK-1)
      XS(IM,KK,L)=XS(IM,KK,1)*((1.-DOLD/DNEW)/(1.-DOLD/DD(KK,L)))**2
      TAU(IM,KK,L)=SCW(KK,L)*XS(IM,KK,L)+TY
      GO TO 820
834   IF ((KK .EQ. 1) .AND. (L .EQ. 1)) GO TO 836
      IF ( L .NE. 1) GO TO 840
      XS(IM,KK,1)=(TAU(IM,KK-1,NIC)-TAU(IM+1,KK,1)-XS(IM,KK-1,NIC)*
     1 SSH(IM)+ XS(IM+1,KK,1)*SCW(KK,1))/(SCW(KK,1)-SSH(IM))
      TAU(IM,KK,1)=SSH(IM)*(XS(IM,KK,1)-XS(IM,KK-1,NIC))+
     1 TAU(IM,KK-1,NIC)
      GO TO 820
836   XS(IM,KK,1)=(-TAU(IM+1,KK,1)+XS(IM+1,KK,1)*SCW(KK,1))/(SCW(KK,1)
     1 -SSH(IM))
      TAU(IM,KK,1)=SSH(IM)*XS(IM,KK,1)
      GO TO 820
840   IF (L .GT. 2) GO TO 843
      DELD=DD(KK,3)-DD(KK,2)
      IF(KK .EQ. 1) GO TO 841
      DOLD=DD(KK-1,NIC)
      GO TO 8411
841   DOLD=DI
8411  DSTAR=DD(KK,1)
      DO 842 LL=1,NIC
      ETA(LL)=FETA(TAU(IM+1,KK,LL),TAU(IM,KK,1),SCW(KK,LL),
     1 XS(IM+1,KK,LL),XS(IM,KK,1))
842   CONTINUE
843   SUM=0.
      DO 845 LL=1,L
      SUM=SUM+ETA(LL)
845   CONTINUE
      XIETA=(SUM-.5*(ETA(L)+ETA(1)))*DELD
      IF (L .EQ. NIC) GO TO 820
      XS(IM,KK,L)=((DOLD*DD(KK,L)**2)/((1.-EPS)*(DD(KK,L)-DOLD)
     1 *WI(KK)*DD(KK,1)))*(ETA(L)-(1./(DD(KK,L)-DOLD))*XIETA)
     2 +XS(IM,KK,1)
      TAU(IM,KK,L)=SCW(KK,L)*(XS(IM,KK,L)-XS(IM+1,KK,L))+
     1 TAU(IM+1,KK,L)
      GO TO 820
846   IF (IM .LT. KK) GO TO 900
      IF (L .NE. 1) GO TO 847
      IF (KK .EQ. 1) GO TO 8461
      XS(IM,KK,1)=(TAU(IM,KK-1,NIC)-TAU(IM+1,KK,1)-XS(IM,KK-1,NIC)*
     1 SSH(IM) +XS(IM+1,KK,1)*SCW(KK,1))/(SCW(KK,1)-SSH(IM))
      TAU(IM,KK,1)=SSH(IM)*(XS(IM,KK,1)-XS(IM,KK-1,NIC))+
     1 TAU(IM,KK-1,NIC)
      GO TO 820
8461  XS(IM,KK,1)=(-TAU(IM+1,KK,1)+XS(IM+1,KK,1)*SCW(KK,1))/
     1 (SCW(KK,1)-SSH(IM))
      TAU(IM,KK,1)=SSH(IM)*XS(IM,KK,1)
      GO TO 820
847   IF (L .GT. 2) GO TO 8481
      DELD=DD(KK,3)-DD(KK,2)
      DO 848 LL=1,NIC
      ETA(LL)=FETA(TAU(IM+1,KK,LL),TAU(IM,KK,1),SCW(KK,LL),
```

```
     1 XS(IM+1,KK,LL),XS(IM,KK,1))
848   CONTINUE
8481  SUM=0.
      DO 849 LL=1,L
      SUM=SUM+ETA(LL)
849   CONTINUE
      XIETA=(SUM-.5*(ETA(L)+ETA(1)))*DELD
      DNEW=DD(KK,L)-DD(KK,NIC)*WI(KK)/OMNEW
      XS(IM,KK,L)=XS(IM,KK,1)+(DD(KK,L)**2/((1.-EPS)*OMNEW*DNEW))*
     1 (ETA(L)-(1./DNEW)*XIETA)
      TAU(IM,KK,L)=SCW(KK,L)*(XS(IM,KK,L)-XS(IM+1,KK,L))+
     1 TAU(IM+1,KK,L)
      GO TO 820
850   CONTINUE
      XMAX=XS(1,1,NIC-1)
      DO 860 L=1,M-1
      IF (XS(L+1,L+1,NIC-1) .GT. XMAX) XMAX=XS(L+1,L+1,NIC-1)
860   CONTINUE
      XMAX=XMAX+1.
      DO 890 L=1,M
      TAU(L,L,NIC)=TAU(L,L,NIC-1)+SSH(L)*(XMAX-XS(L,L,NIC-1))
      TAUA(L)=TAU(L-1,L,NIC)+SCW(L,NIC)*(XMAX-XS(L-1,L,NIC))
      DEGA(L)=ROT*TAUA(L)*50./(V*60.)
      XS(L,L,NIC)=XMAX
890   CONTINUE
      IF (IM .EQ. KK) GO TO 895
      WRITE(6,1550) IM,KK
      WRITE(6,1600) (DD(KK,L),L=1,NIC)
      WRITE(6,1620) KK,IM
      WRITE(6,1625) (SCW(KK,L),L=1,NIC)
895   WRITE(6,1630) SSH(IM)
900   CONTINUE
950   CONTINUE
D     WRITE(6,1650) XDATE,XTIME
      WRITE(6,1660)
      DO 980 I=M,1,-1
      DO 970 KK=1,M
      IF (KK .GT. I) GO TO 980
      DO 960 L=1,NIC
      DEG(I,KK,L)=ROT*TAU(I,KK,L)*50./(V*60.)
      WRITE(6,1700) I,KK,L,XS(I,KK,L),TAU(I,KK,L),DEG(I,KK,L)
960   CONTINUE
970   CONTINUE
980   CONTINUE
1450  FORMAT(////T10,'ISOCONCENTRATIONS AFTER INTERACTION WITH SHOCK
     1 WAVE NO.',I2,//T20,'WAVE NO.',T30,'L',T35,'M:',/)
1500  FORMAT(T23,I2,T30,I1,T33,6E13.3)
1550  FORMAT(////T10,'NEW D''S AFTER SHOCK NO.',I2,' WAVE NO.',
     1 I2,/)
1600  FORMAT(T30,5E13.3,/T30,5E13.3)
1620  FORMAT(////T10,'NEW C-WAVE SLOPES:',I2,' WAVE AFTER',I2,
     1 ' SHOCK',/)
1625  FORMAT(T30,5E13.3,/T30,5E13.3)
1630  FORMAT(////T10,'NEW SHOCK WAVE SLOPE',/T30,E13.3)
```

```
1650  FORMAT('1',/T10,9A1,3X,8A1)
1660  FORMAT(///T10,'COORDINATES OF INTERSECTIONS
     1 OF C-WAVES AND SHOCK WAVES',/T10,57('*'),/T20,'SHOCK NO.',T30,
     2 'WAVE NO.',T40,'L',T55,'X',T65,'TAU',T75,'DEGREES ROT.',/)
1700  FORMAT(T23,I1,T33,I1,T40,I1,T50,F10.4,T60,F10.4,T70,F10.2)
      RETURN
      END



      FUNCTION FETA(U,V,W,X,Y)
      FETA=U-V-W*(X-Y)
      RETURN
      END
```

```
      SUBROUTINE PLOTDT
      LOGICAL*1 XTIME(8),XDATE(9)
      DIMENSION Y(6,6,8),X(6,6,8),DEGA(6)
      COMMON /BLK1/MINX,MAXX,MINY,MAXY
      COMMON /BLK2/XDATE,XTIME
      COMMON /BLK4/ Y,X,NSOL,NIC,YI,DEGA
      ICNT=0
      TYPE 100
100   FORMAT(' DO YOU WANT A PLOT? (0=NO; 1=YES)',$)
      MINX=150
      MAXX=900
      MINY=150
      MAXY=700
      ACCEPT 150,IA
150   FORMAT(I2)
      IF (IA .EQ. 0) RETURN
50    CALL INITT(480)
      ICNT=ICNT+1
      TYPE 60
60    FORMAT(' ENTER XMAX AND YMAX IN F8.4 FORMAT.')
      ACCEPT 70, XMAX,YMAX
70    FORMAT(2F8.4)
      CALL TWINDO(MINX,MAXX,MINY,MAXY)
      CALL DWINDO(0.,XMAX,0.,YMAX)
C
C         DRAW SHOCK WAVES
C
      CALL MOVEA(0.,0.)
      DO 300 I=NSOL,1,-1
      DO 200 J=1,NSOL
      IF (J .GT. I) GO TO 260
      DO 180 K=1,NIC
      CALL DASHA(X(I,J,K),Y(I,J,K),I)
180   CONTINUE
200   CONTINUE
260   CALL MOVEA(0.,0.)
300   CONTINUE
C
C         DRAW C-WAVES
C
      CALL MOVEA(0.,YI)
      DO 800 J=1,NSOL
      K=NIC
      DO 600 I=NSOL,1,-1
      IF (J .GT. I) GO TO 600
      IF ((I .EQ. J) .AND. (K .EQ. NIC)) GO TO 550
      CALL DASHA(X(I,J,K),Y(I,J,K),J)
      GO TO 600
550   CALL DASHA(X(NSOL,NSOL,NIC),DEGA(J),J)
600   CONTINUE
      CALL MOVEA(0.,YI)
800   CONTINUE
      CALL GRID(0.,XMAX,0.,YMAX)
      IXO=MINX
```

```
      IYO=730
      CALL MOVABS(IXO,IYO)
      CALL ANMODE
      WRITE(1,900) XDATE,XTIME,ICNT
900   FORMAT(1H+,$,9A1,3X,8A1,5X,'GRAPH NO.',I2)
      TYPE 1000
1000  FORMAT(' DO YOU WANT ANOTHER PLOT WITH DIFFERENT SCALING? (0=NO;
     1 1=YES):',$)
      ACCEPT 1100, IA
1100  FORMAT(I2)
      IF (IA .NE. 0) GO TO 50
      RETURN
      END
```

```
      SUBROUTINE GRID(XMIN,XMAX,YMIN,YMAX)
      COMMON /BLK1/MINX,MAXX,MINY,MAXY
      IDELY=(MAXY-MINY)/5
      IDELX=(MAXX-MINX)/5
      CALL MOVABS(MINX,MINY)
      IX=MINX
      DO 100 I=1,6
      CALL DRWABS(IX,MAXY)
      IX=IX+IDELX
      CALL MOVABS(IX,MINY)
100   CONTINUE
      IY=MINY
      CALL MOVABS(MINX,MINY)
      DO 200 I=1,6
      CALL DRWABS(MAXX,IY)
      IY=IY+IDELY
      CALL MOVABS(MINX,IY)
200   CONTINUE
      CALL CSIZE(IHORZ,IVERT)
      IXEXP=ALOG10(XMAX)
      IYEXP=ALOG10(YMAX)
      XMAXN=XMAX/(10**IXEXP)
      XMINN=XMIN/(10**IXEXP)
      YMINN=YMIN/(10**IYEXP)
      YMAXN=YMAX/(10**IYEXP)
      DELX=(XMAXN-XMINN)/5.
      DELY=(YMAXN-YMINN)/5.
      IXO=MINX-2*IHORZ
      IYO=MINY-1.5*IVERT
      CALL MOVABS(IXO,IYO)
      X=XMINN
      DO 300 I=1,6
      CALL ANMODE
      WRITE(1,1000) X
      X=X+DELX
      IXO=IXO+IDELX
      CALL MOVABS(IXO,IYO)
1000  FORMAT(1H+,$,F4.2)
300   CONTINUE
      IXO=MAXX-7*IHORZ
      IYO=IYO-2*IVERT
      IXEXP=-IXEXP
      IYEXP=-IYEXP
      CALL MOVABS(IXO,IYO)
      CALL ANMODE
      WRITE(1,1100) IXEXP
1100  FORMAT(1H+,$,'X10**',I2)
      IXO=MINX-4*IHORZ
      IYO=MINY-.5*IVERT
      CALL MOVABS(IXO,IYO)
      Y=YMINN
      DO 400 I=1,6
      CALL ANMODE
      WRITE(1,1200) Y
```

```
1200  FORMAT(1H+,$,F4.2)
      Y=Y+DELY
      IYO=IYO+IDELY
      CALL MOVABS(IXO,IYO)
400   CONTINUE
      IYO=MAXY-2*IVERT
      IXO=MINX-7*IHORZ
      CALL MOVABS(IXO,IYO)
      CALL ANMODE
      WRITE(1,1300) IYEXP
1300  FORMAT(1H+,$,'X10**',I2)
      RETURN
      END
```

```
      SUBROUTINE INSECT
      REAL*4 K(6),N
      LOGICAL*1 XDATE(9),XTIME(8)
      DIMENSION D(6),SSH(6),DD(6,8),PHI(6,6,6,8),XS(6,6,8),
     1 TAU(6,6,8),WI(6),WE(6), SCW(6,8),PHICS(6,6),TAUA(6),
     1 DEG(6,6,8), DEGA(6),TI(72),PHICON(72,6),DEE(72),PHICSN(6,6)
      COMMON TY,SSH,SCW,TAU,DD,D,WE,WI,EPS,PHI,N,K,DI,DE,TAUA
     1 ,V,ROT
      COMMON /BLK2/ XDATE,XTIME
      COMMON /BLK3/ XISO,PHICS,DEE,PHICON,ICNT
      COMMON /BLK4/ DEG,XS,M,NIC,TYD,DEGA
C
C         FIND INTERSECTIONS WITH SHOCK WAVES
C
      TYPE 2600
      ACCEPT 2700, XISO
      ICNT=0
      DO 200 KK=1,M
      DO 100 I=1,M
      PHICSN(I,KK)=PHICS(I,KK)
100   CONTINUE
200   CONTINUE
      DO 900 I=1,M
      DO 850 KK=1,M
      IF (KK .GT. I) GO TO 850
      DO 800 L=1,NIC
      IF (XISO .GT. XS(I,KK,L)) GO TO 800
      ICNT=ICNT+1
      XRT=XS(I,KK,L)
      TRT=TAU(I,KK,L)
      IF ((KK .EQ. 1) .AND. (L .EQ. 1)) GO TO 790
      IF ( L .EQ. 1) GO TO 785
      XLT=XS(I,KK,L-1)
      TLT=TAU(I,KK,L-1)
      GO TO 795
785   XLT=XS(I,KK-1,NIC)
      TLT=TAU(I,KK-1,NIC)
      GO TO 795
790   XLT=0.
      TLT=0.
795   TI(ICNT)=(XISO-XLT)*(TLT-TRT)/(XLT-XRT)+TLT
      IF (I .EQ. 1) GO TO 7958
      DO 7955 KK=1,I-1
      IF (XISO .LT. XS(I,KK,NIC)) GO TO 7956
      PHICSN(KK,I-1)=0.
      PHICSN(KK,I)=0.
      GO TO 7955
7956  IF (XISO .LT. XS(I,KK,1)) GO TO 7958
C
C     XISO INTERSECTS BETWEEN L==1 AND L=NIC
C
      DO 7957 KKK=KK,I-1
      PHICSN(KKK,I-1)=(XISO-XLT)*(PHI(I-1,KKK,KKK,L)-
     1 PHI(I-1,KKK,KKK,L-1))/ (XRT-XLT) + PHI(I-1,KKK,KKK,L-1)
```

```
      PHICSN(KKK,I)=(XISO-XLT)*(PHI(I,KKK,KKK,L)-PHI(I,KKK,KKK,L-1))/
     1 (XRT-XLT) + PHI(I,KKK,KKK,L-1)
7957  CONTINUE
7955  CONTINUE
7958  DO 796 MM=1,M
      IF (I .EQ. 1) GO TO 7995
      PHICON(ICNT,MM)=PHICSN(MM,I-1)
      GO TO 796
7995  PHICON(ICNT,MM)=0.
796   CONTINUE
      ICNT=ICNT+1
      TI(ICNT)=TI(ICNT-1)
      DO 799 MM=1,M
      PHICON(ICNT,MM)=PHICSN(MM,I)
799   CONTINUE
      GO TO 900
800   CONTINUE
850   CONTINUE
900   CONTINUE
C
C         FIND INTERSECTIONS WITH C-WAVES
C
      DO 990 KK=1,M
      DO 980 L=1,NIC
      DO 970 I=M,1,-1
      IF (I .LT. KK) GO TO 970
      IF (XISO .GT. XS(I,KK,L)) GO TO 970
      ICNT=ICNT+1
      XRT=XS(I,KK,L)
      TRT=TAU(I,KK,L)
      IF (I .EQ. M) GO TO 950
      XLT=XS(I+1,KK,L)
      TLT=TAU(I+1,KK,L)
      GO TO 960
950       XLT=0.
      TLT=TY
960   TI(ICNT)=(XISO-XLT)*(TLT-TRT)/(XLT-XRT)+TLT
      DO 966 MM=1,M
      PHICON(ICNT,MM)=PHI(I,MM,KK,L)
966   CONTINUE
      GO TO 980
970   CONTINUE
980   CONTINUE
990    CONTINUE
C
C         PUT TI'S IN ASCENDING ORDER
C
      IEND=ICNT-1
      DO 999 I=1,IEND
      DO 997 J=1,I
      II=I-J+1
      IF (TI(II+1) .GE. TI(II)) GO TO 997
      TSAV=TI(II)
      TI(II)=TI(II+1)
```

```
      TI(II+1)=TSAV
      DO 995 MM=1,M
      PHISAV=PHICON(II,MM)
      PHICON(II,MM)=PHICON(II+1,MM)
      PHICON(II+1,MM)=PHISAV
995   CONTINUE
997   CONTINUE
999   CONTINUE
      WRITE(6,2750) XDATE,XTIME,XISO
      DO 998 I=1,ICNT
      DEE(I)=ROT*TI(I)*50./(V*60.)
      WRITE(6,2800) TI(I),DEE(I),(PHICON(I,MM),MM=1,M)
998   CONTINUE
      RETURN
2600  FORMAT(' ENTER THE DIMENSIONLESS BED LENGTH DESIRED IN F8.4
     1FORMAT.')
2700  FORMAT(F8.4)
2750  FORMAT('1',/T10,9A1,3X,8A1,//T10,'PROFILE DATA',/T10,11('*'),//T20,
     1 'TAU',T30,'DEGREES',T40,'PHI''S:',T80,
     2 'X=',F5.2,//)
2800  FORMAT(T15,8F10.4)
      END
```

```
      SUBROUTINE PLOTPR(NSOL)
      LOGICAL*1 XTIME(8),XDATE(9)
      DIMENSION X(72),Y(72,6),DUM(6,6)
      COMMON /BLK2/XDATE,XTIME
      COMMON /BLK1/MINX,MAXX,MINY,MAXY
      COMMON /BLK3/ XISO,DUM,X,Y,NPTS
      ICNT=0
50    CALL INITT(480)
      ICNT=ICNT+1
      TYPE 60
60    FORMAT(' ENTER RANGE (MINIMUM AND MAXIMUM) VALUES FOR ANGULAR RO
     1TATION IN 2F8.4 FORMAT.')
      ACCEPT 70, XMIN,XMAX
70    FORMAT(2F8.4)
      TYPE 80
80    FORMAT(' ENTER RANGE (MINIMUM AND MAXIMUM) VALUES OF
     1CONCENTRATIONS IN 2F8.4 FORMAT.')
      ACCEPT 70, YMIN,YMAX
      MINX=150
      MAXX=900
      MINY=150
      MAXY=700
      CALL TWINDO(MINX,MAXX,MINY,MAXY)
      CALL DWINDO(XMIN,XMAX,YMIN,YMAX)
C
C          DRAW CURVES FOREACH SOLUTE
C
      DO 200 I=1,NSOL
      CALL MOVEA(X(1),0.)
      DO 100 J=1,NPTS
      CALL DASHA(X(J),Y(J,I),I)
100   CONTINUE
200   CONTINUE
      CALL GRID(XMIN,XMAX,YMIN,YMAX)
      IXO=MINX
      IYO=730
      CALL MOVABS(IXO,IYO)
      CALL ANMODE
      WRITE(1,300) XDATE,XTIME,XISO,ICNT
300   FORMAT(1H+,$,9A1,3X,8A1,5X,'X=',F4.1,3X,'GRAPH NO.',I2)
      TYPE 1000
1000  FORMAT(' DO YOU WANT ANOTHER PLOT WITH DIFFERENT SCALING?
     1 (0=NO; 1=YES):',$)
      ACCEPT 1100, IA
1100  FORMAT(I2)
      IF (IA .NE. 0) GO TO 50
      RETURN
      END
```

THIS PAGE

WAS INTENTIONALLY

LEFT BLANK

APPENDIX B. GRAPHICAL RESULTS

THIS PAGE

WAS INTENTIONALLY

LEFT BLANK

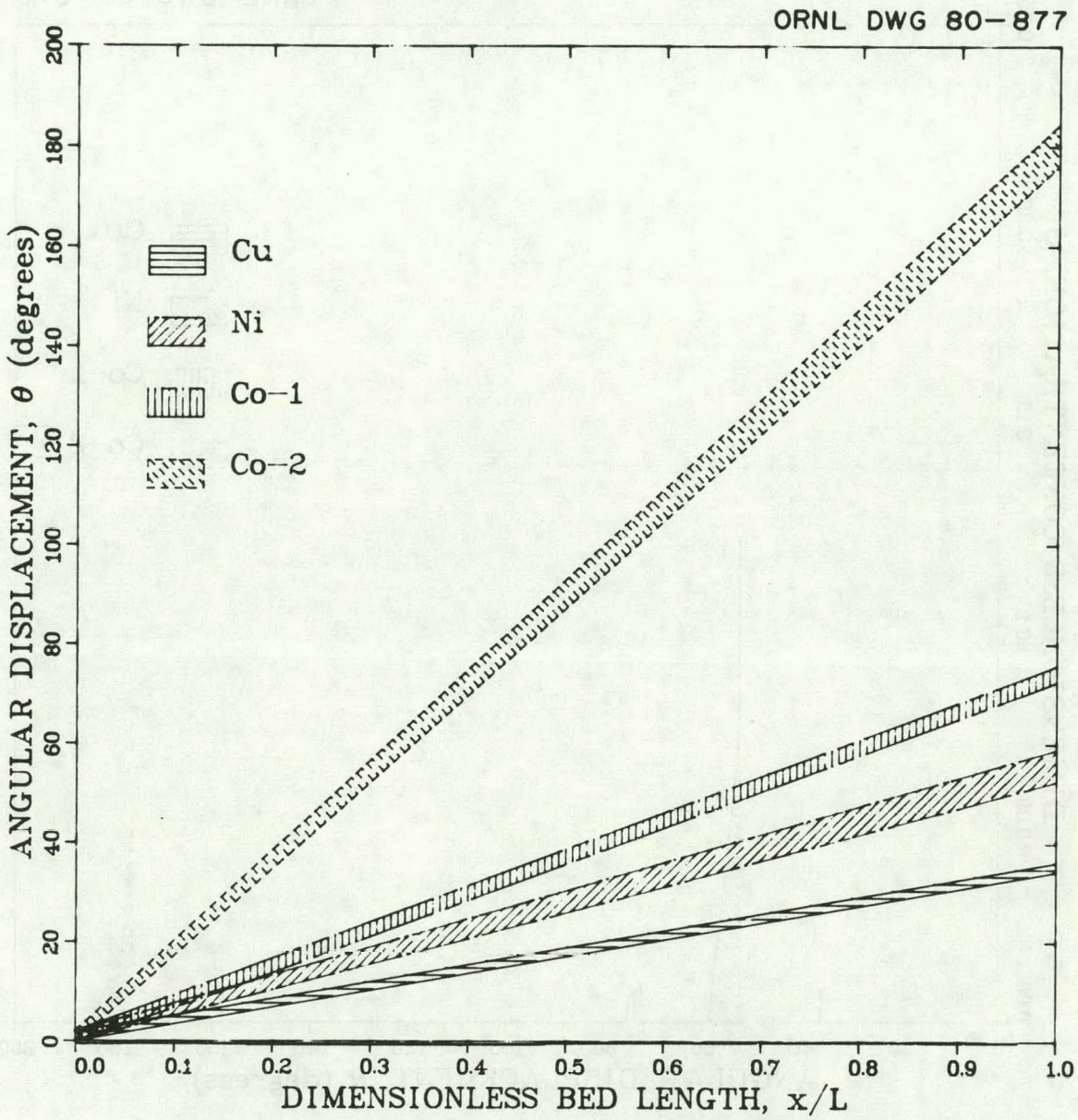

Fig. B.1. Solute bands along the column length for a 5-mm feed bandwidth.

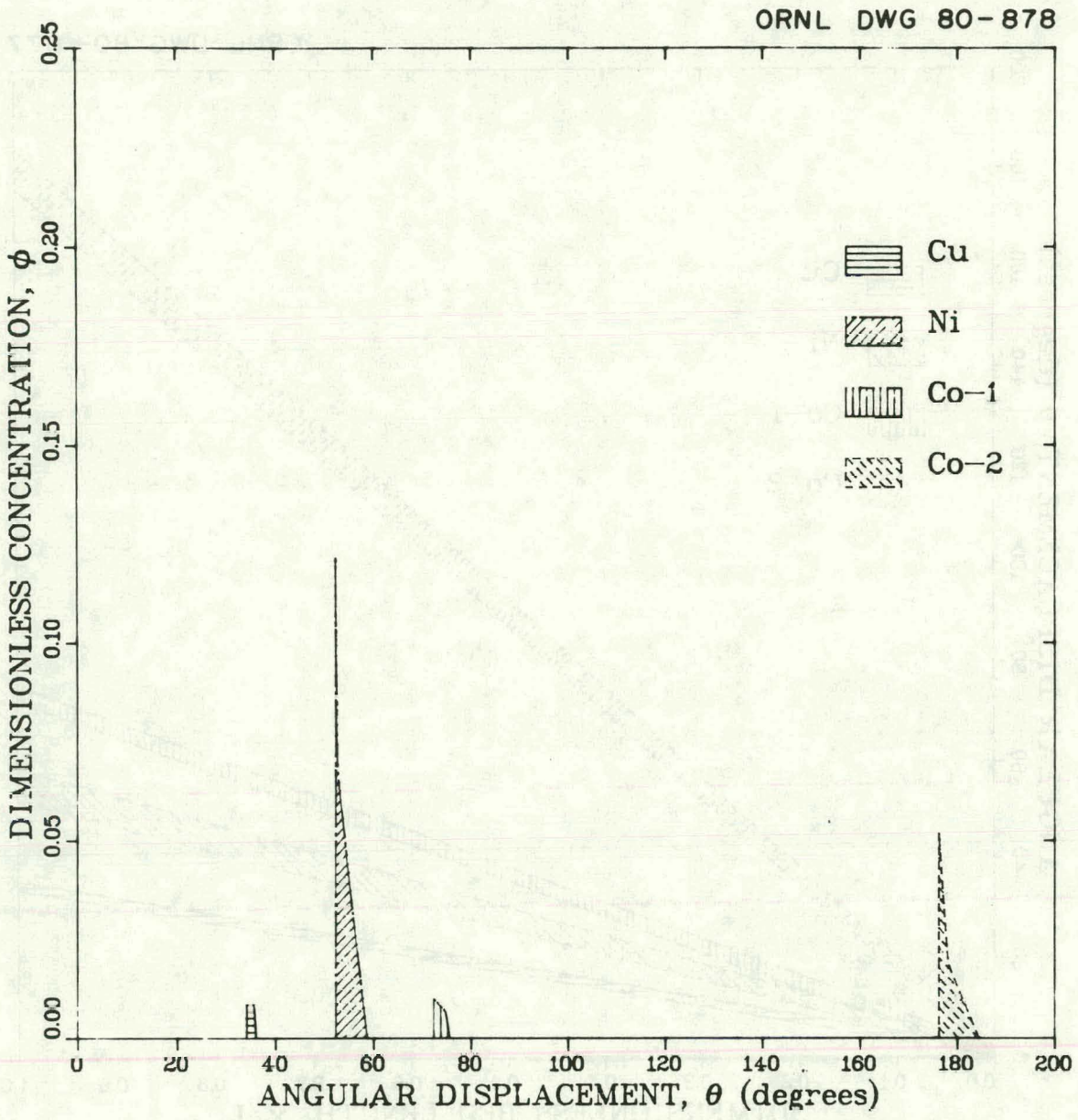

Fig. B.2. Concentration profile at the column exit for a 5-mm feed bandwidth.

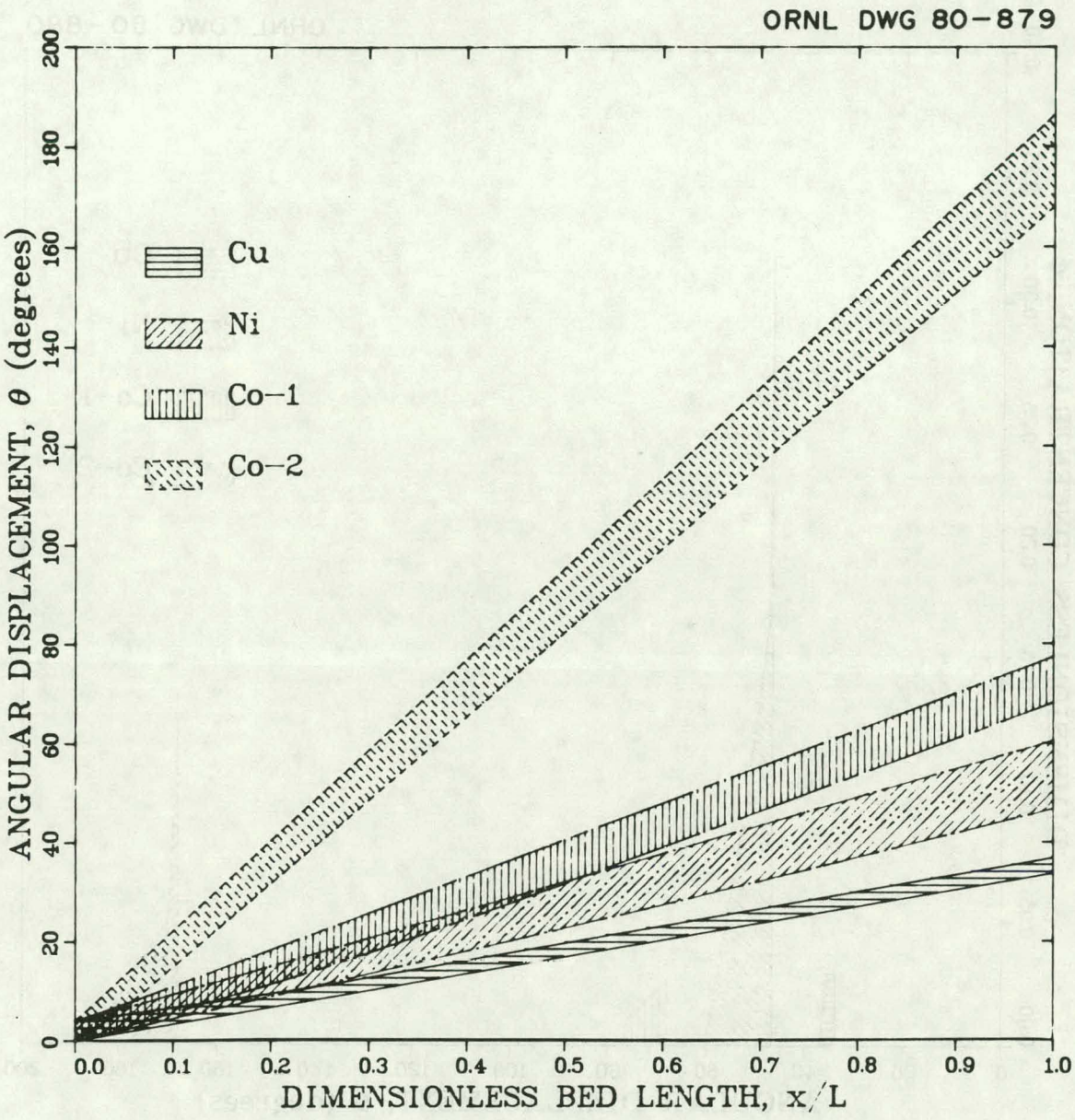

Fig. B.3. Solute bands along the column length for a 10-mm feed bandwidth.

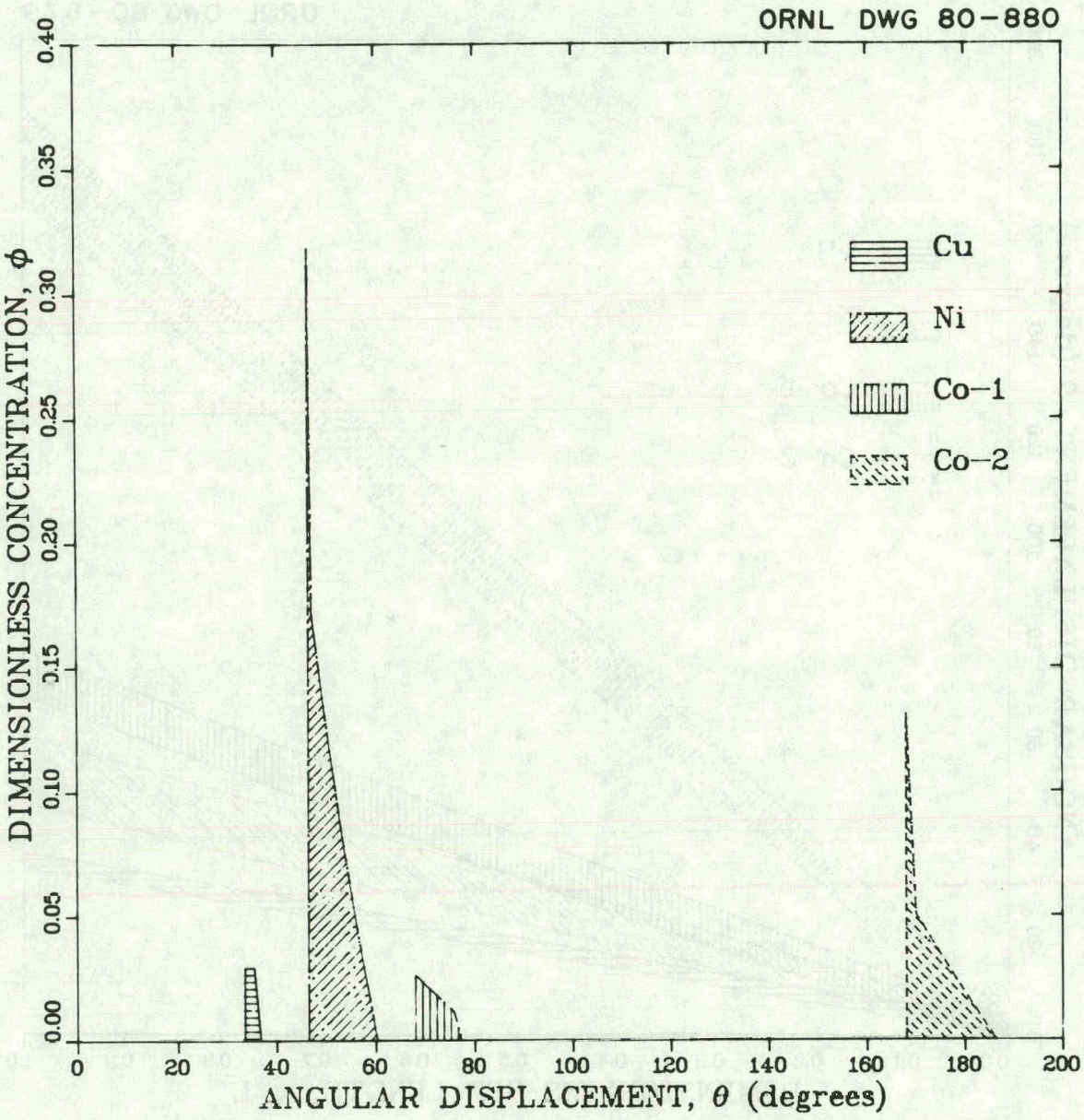

Fig. B.4. Concentration profile at the column exit for a 10-mm feed bandwidth.

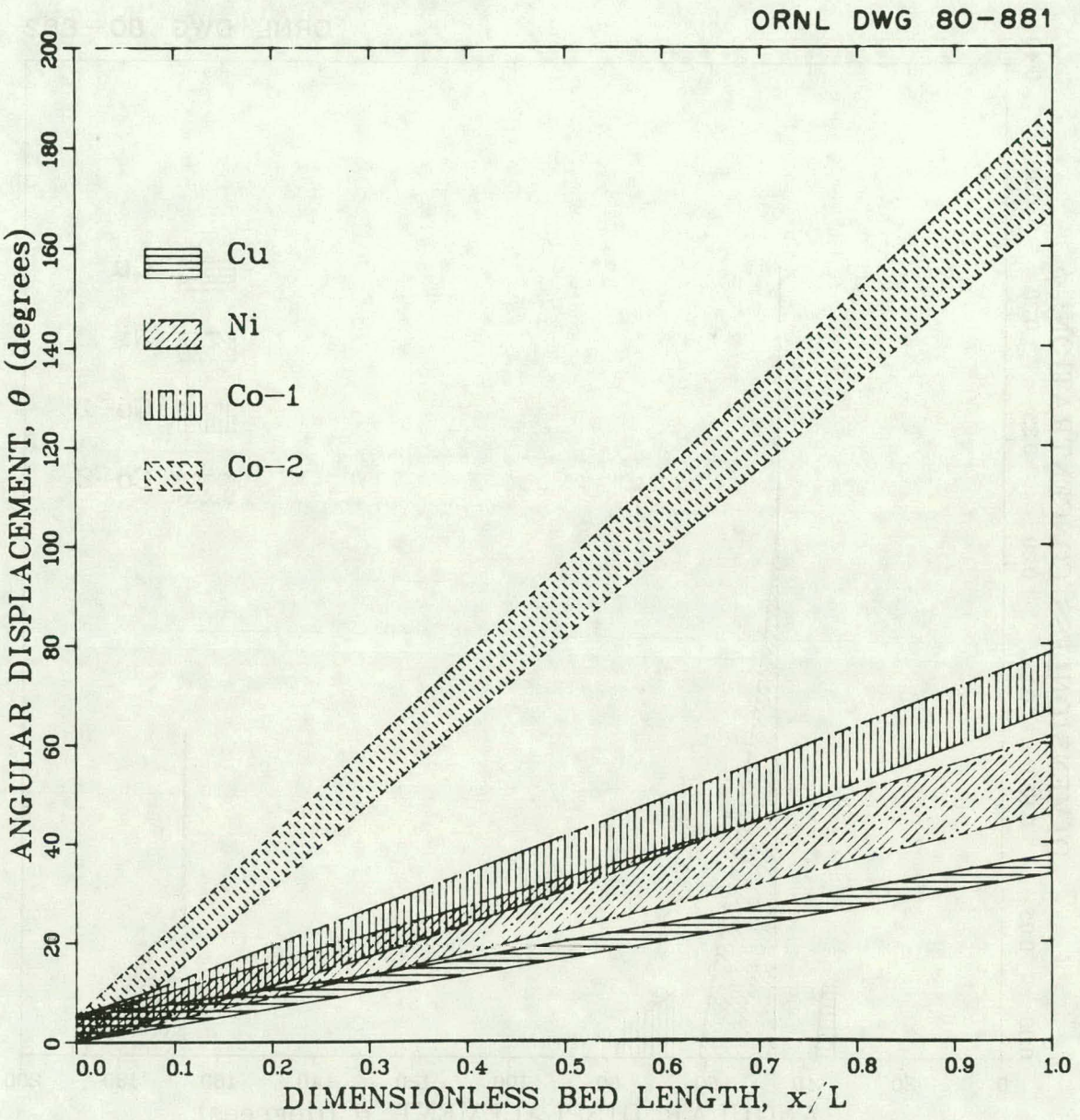

Fig. B.5. Solute bands along the column length for a 13-mm feed bandwidth.

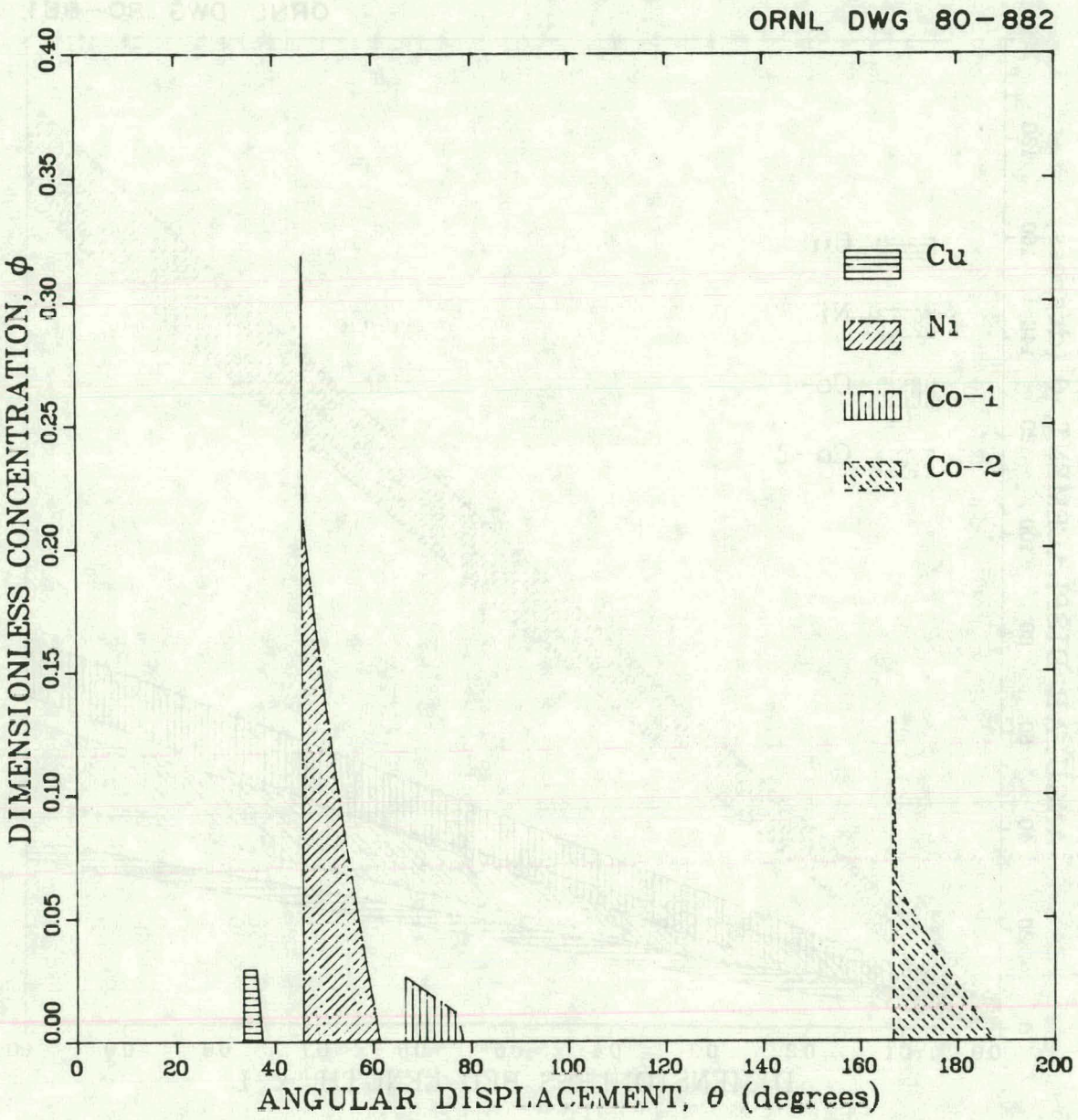

Fig. B.6. Concentration profile at the column exit for a 13-mm feed bandwidth.

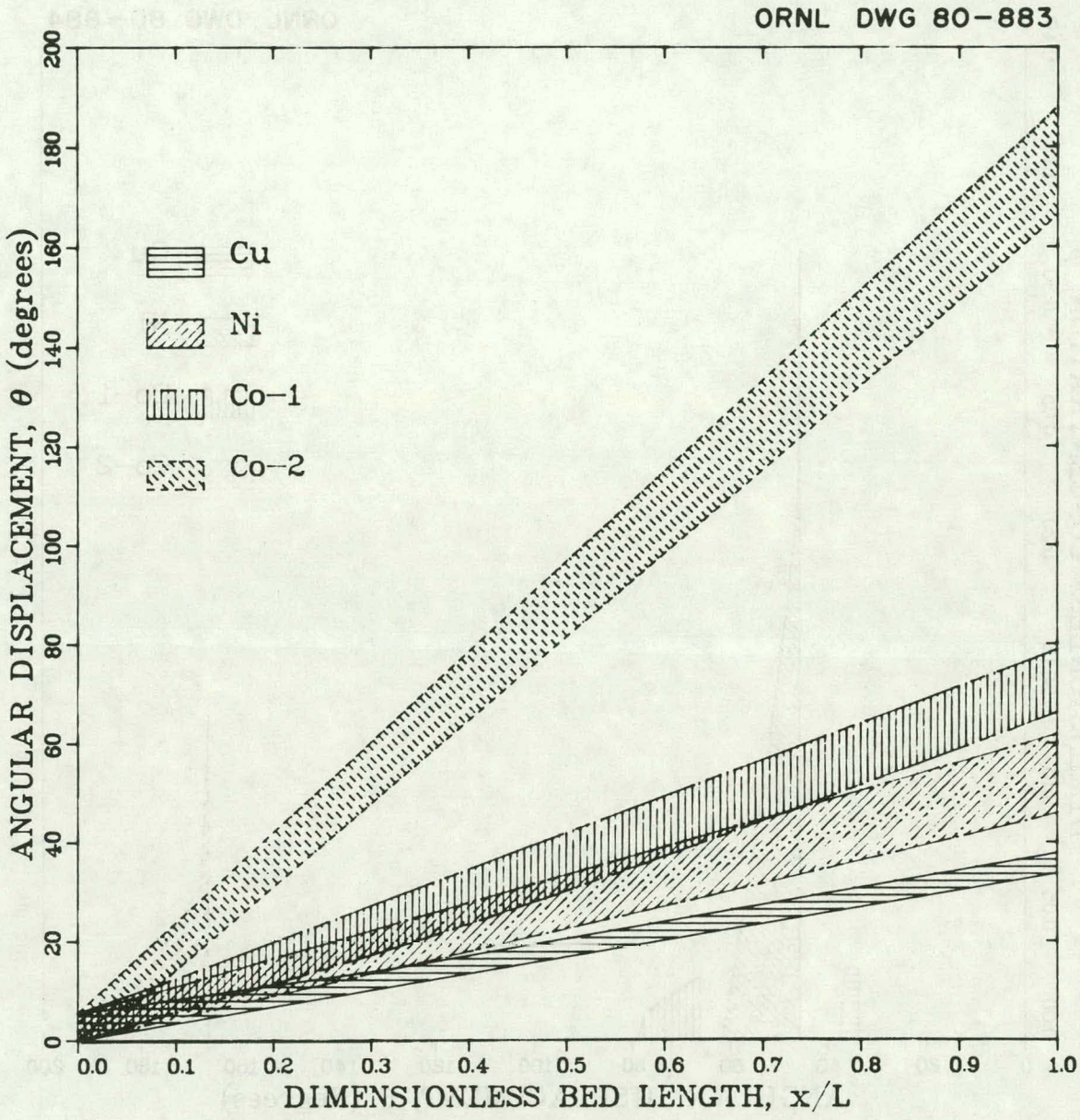

Fig. B.7. Solute bands along the column length for a 14-mm feed bandwidth.

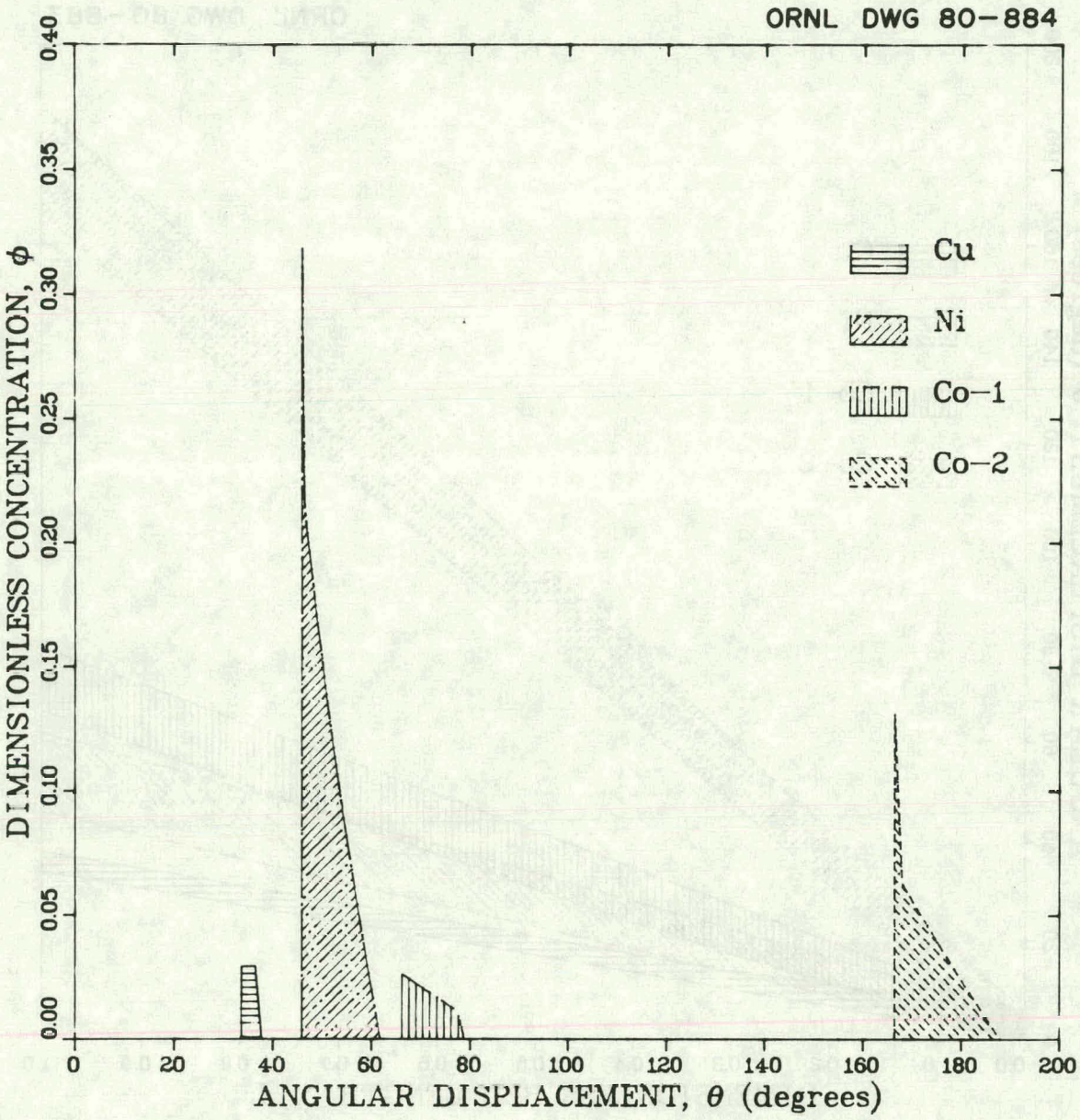

Fig. B.8. Concentration profile at the column exit for a 14-mm feed bandwidth.

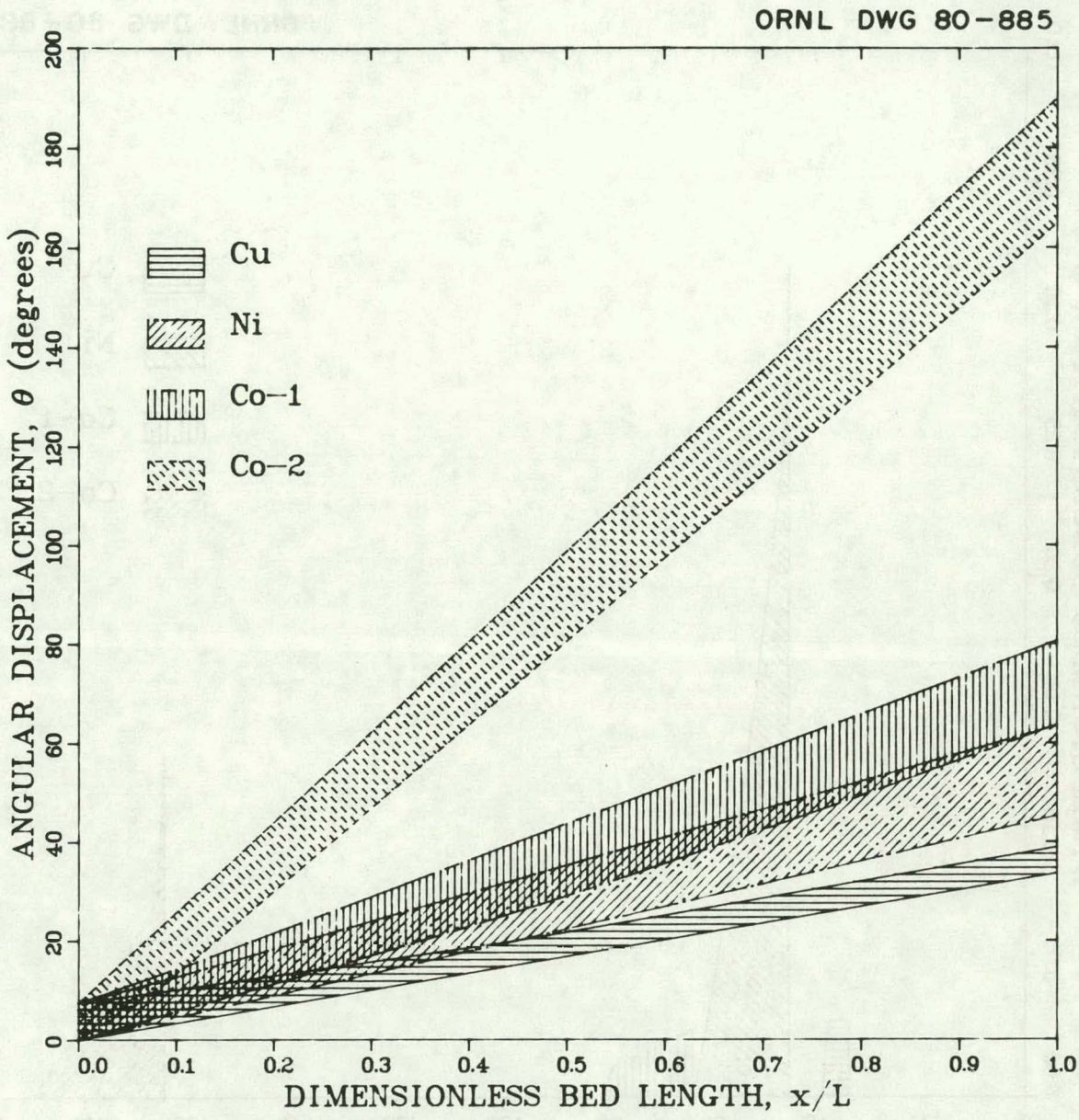

Fig. B.9. Solute bands along the column length for a 19-mm feed bandwidth.

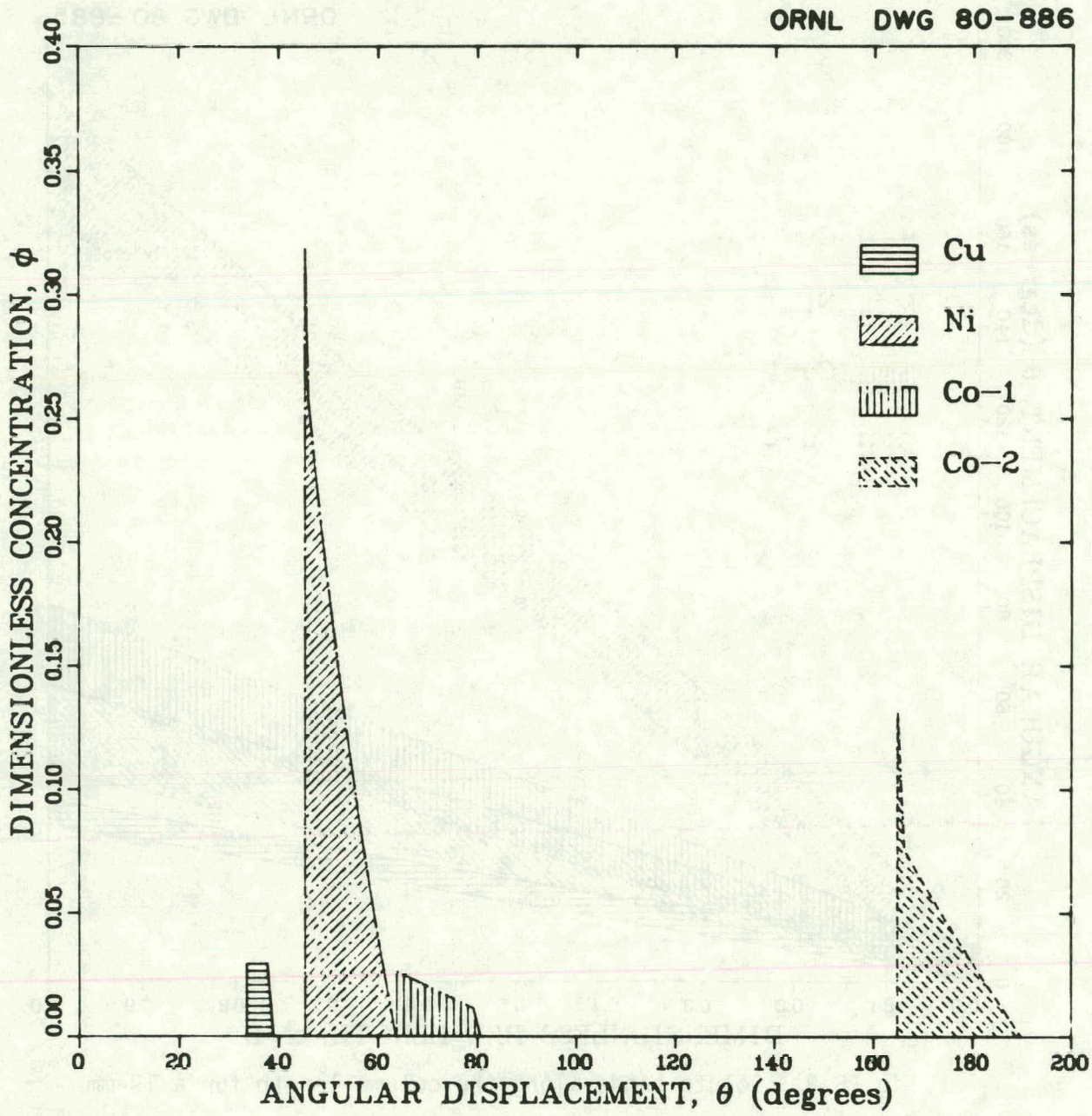

Fig. B.10. Concentration profile at the column exit for a 19-mm feed bandwidth.

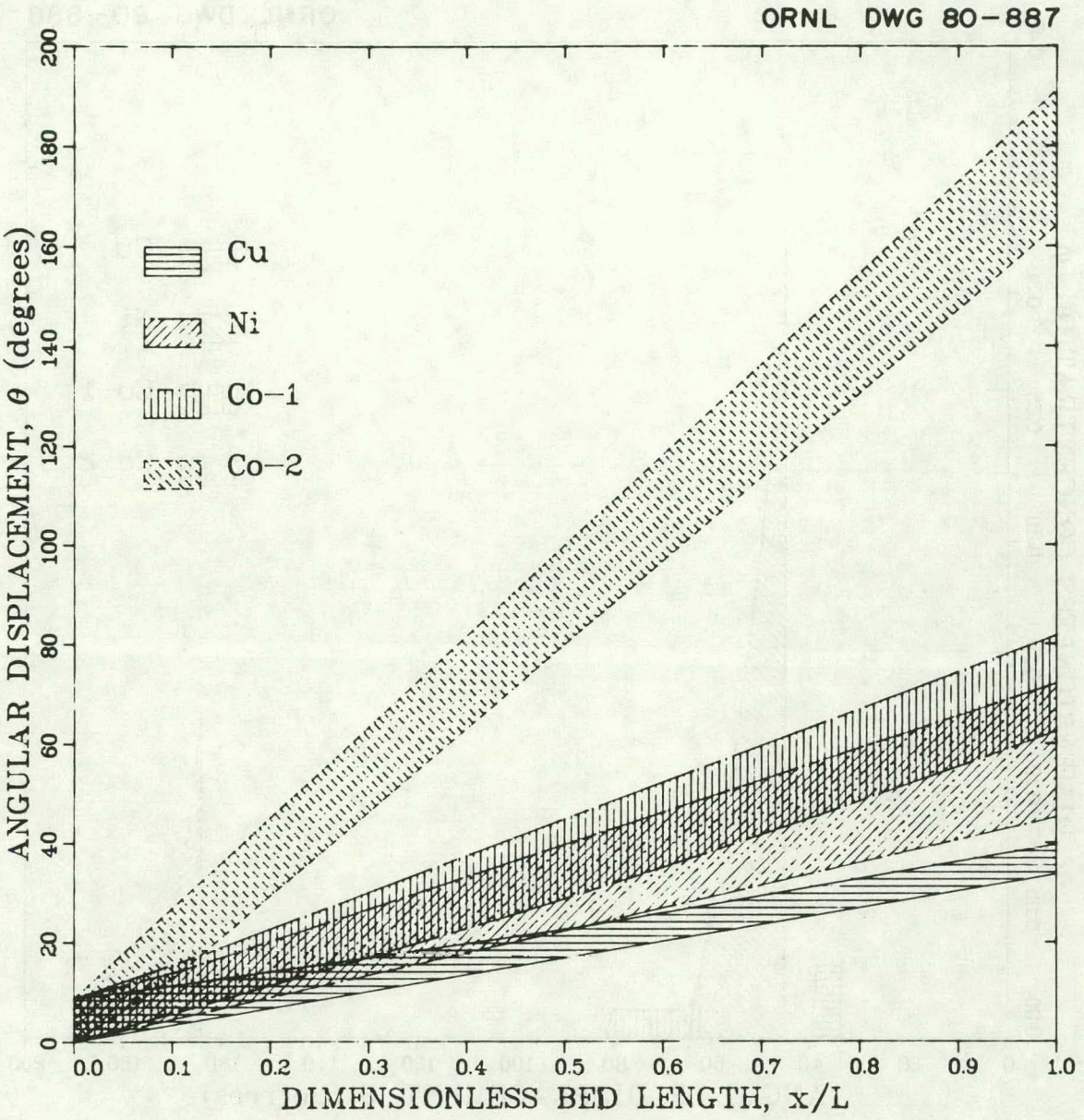

Fig. B.11. Solute bands along the column length for a 22-mm feed bandwidth.

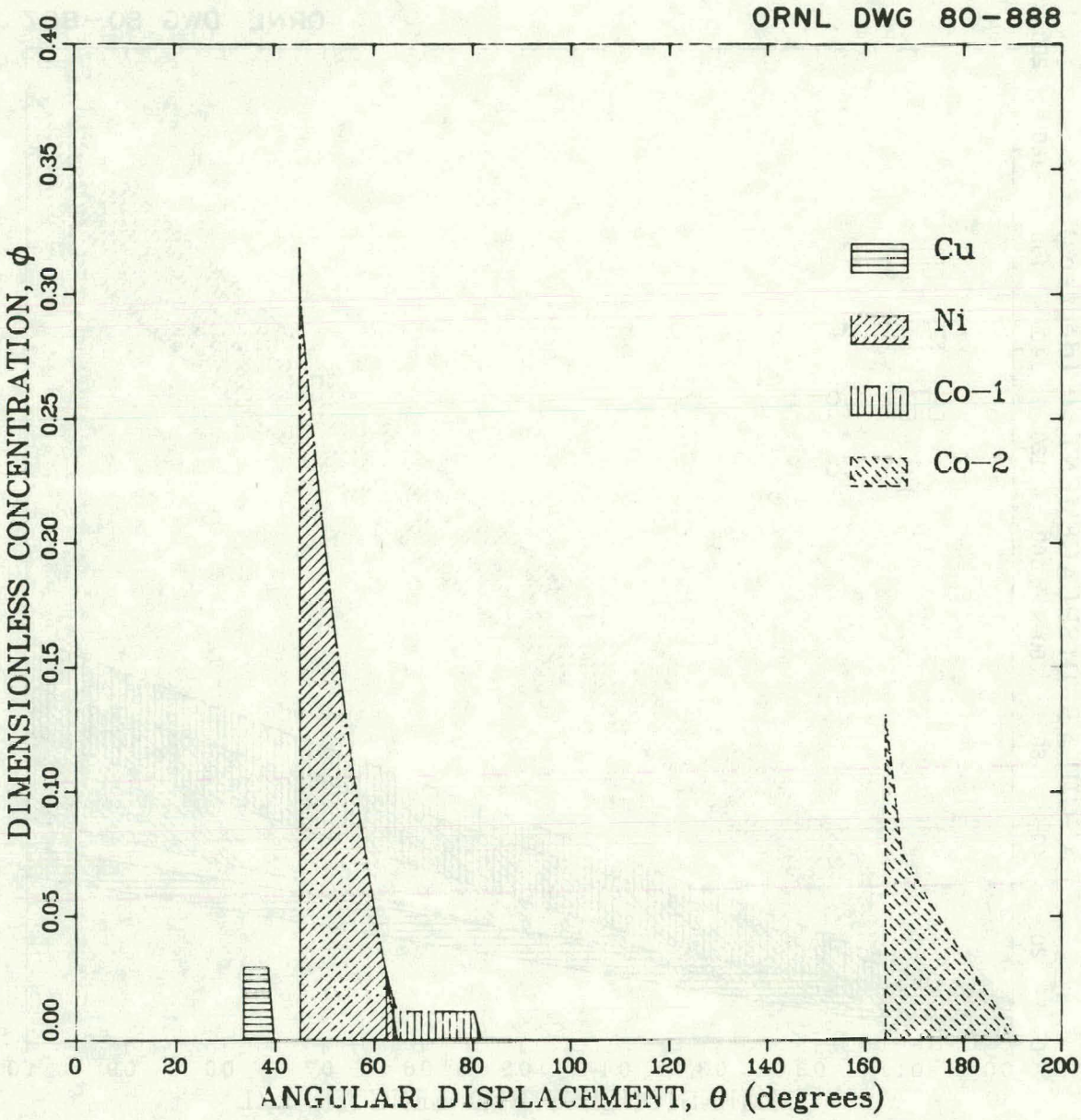

Fig. B.12. Concentration profile at the column exit for a 22-mm feed bandwidth.

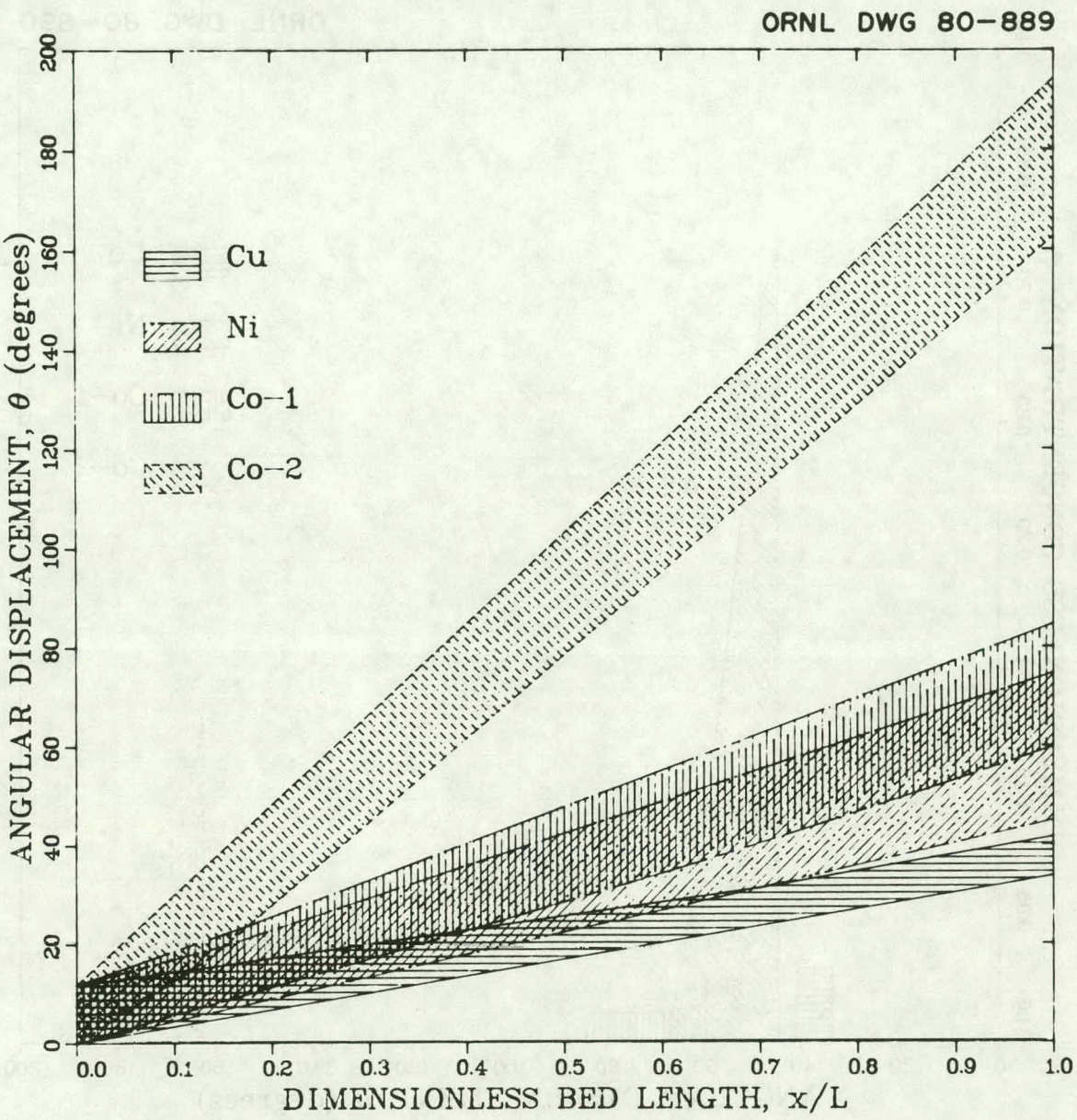

Fig. B.13. Solute bands along the column length for a 30-mm feed bandwidth.

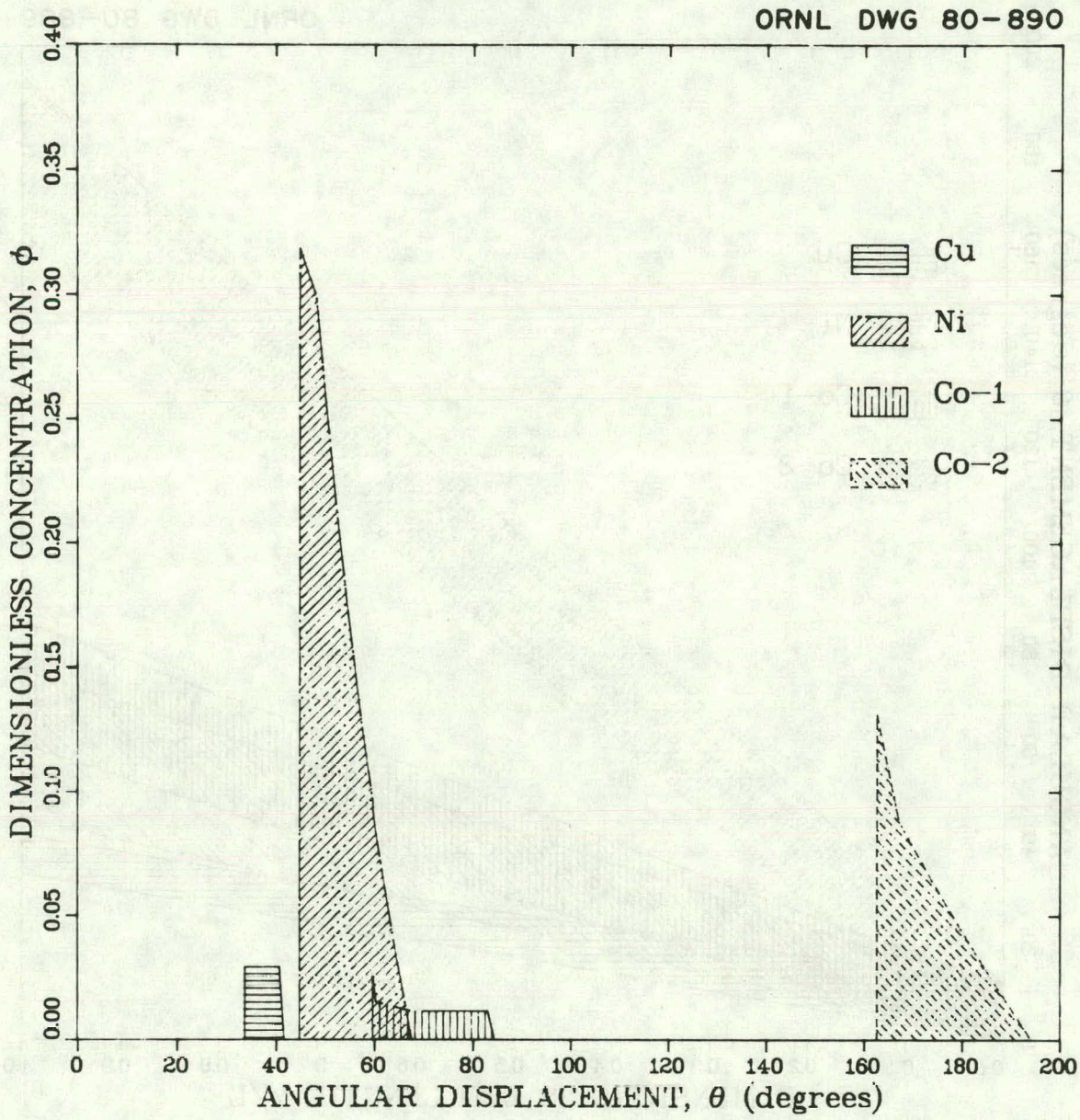

Fig. B.14. Concentration profile at the column exit for a 30-mm feed bandwidth.

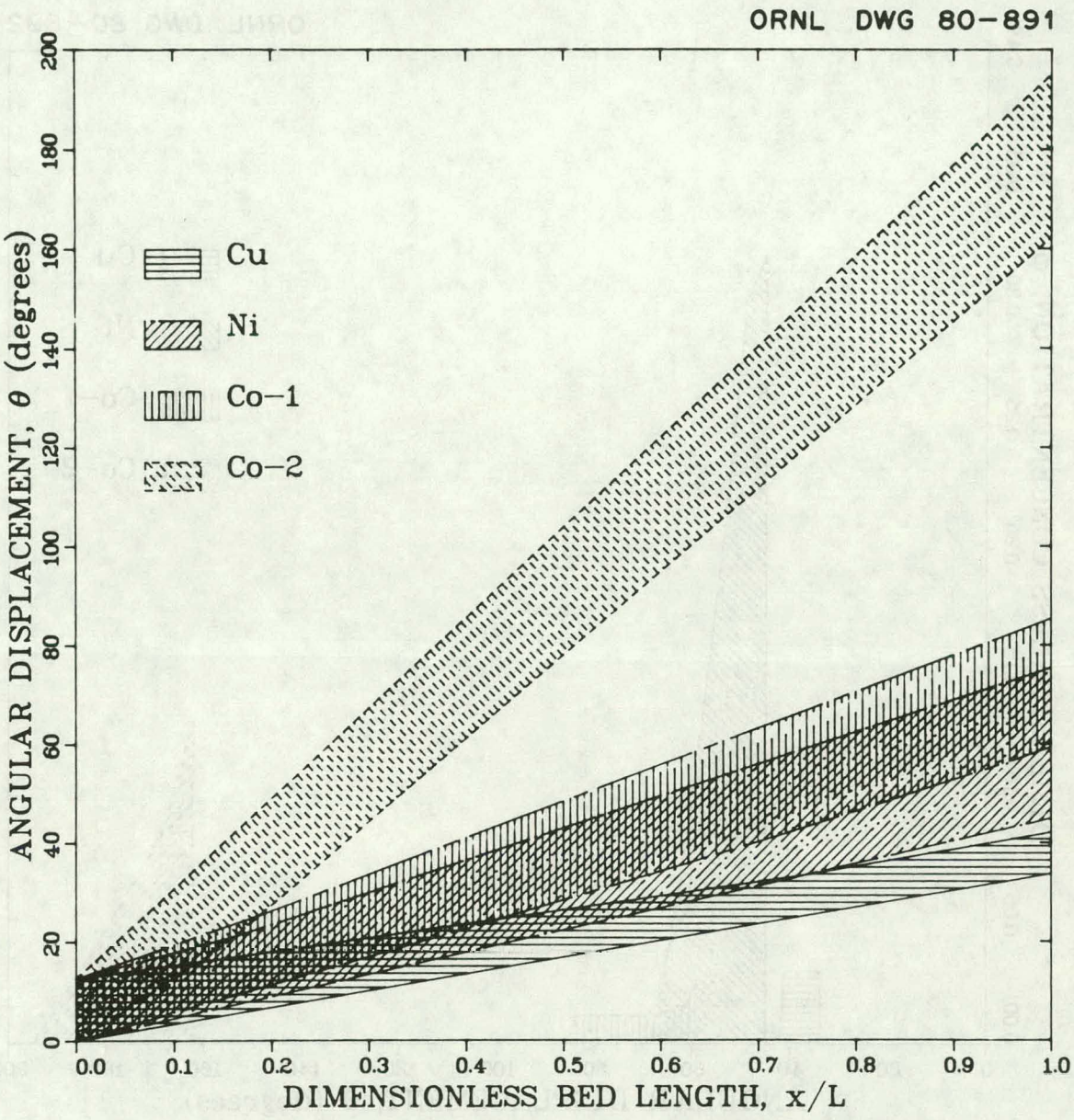

Fig. B.15. Solute bands along the column length for a 32-mm feed bandwidth.

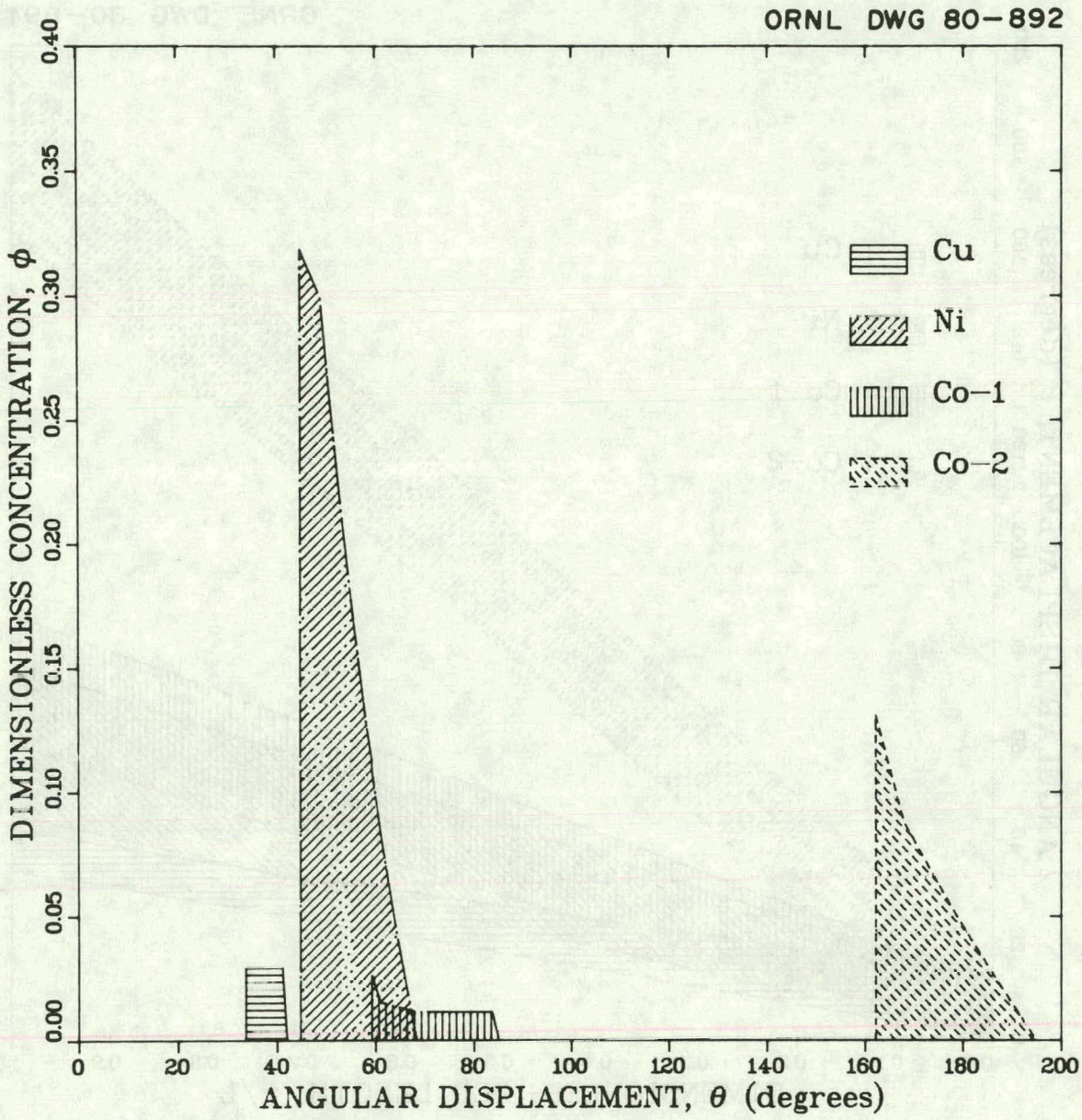

Fig. B.16. Concentration profile at the column exit for a 32-mm feed bandwidth.

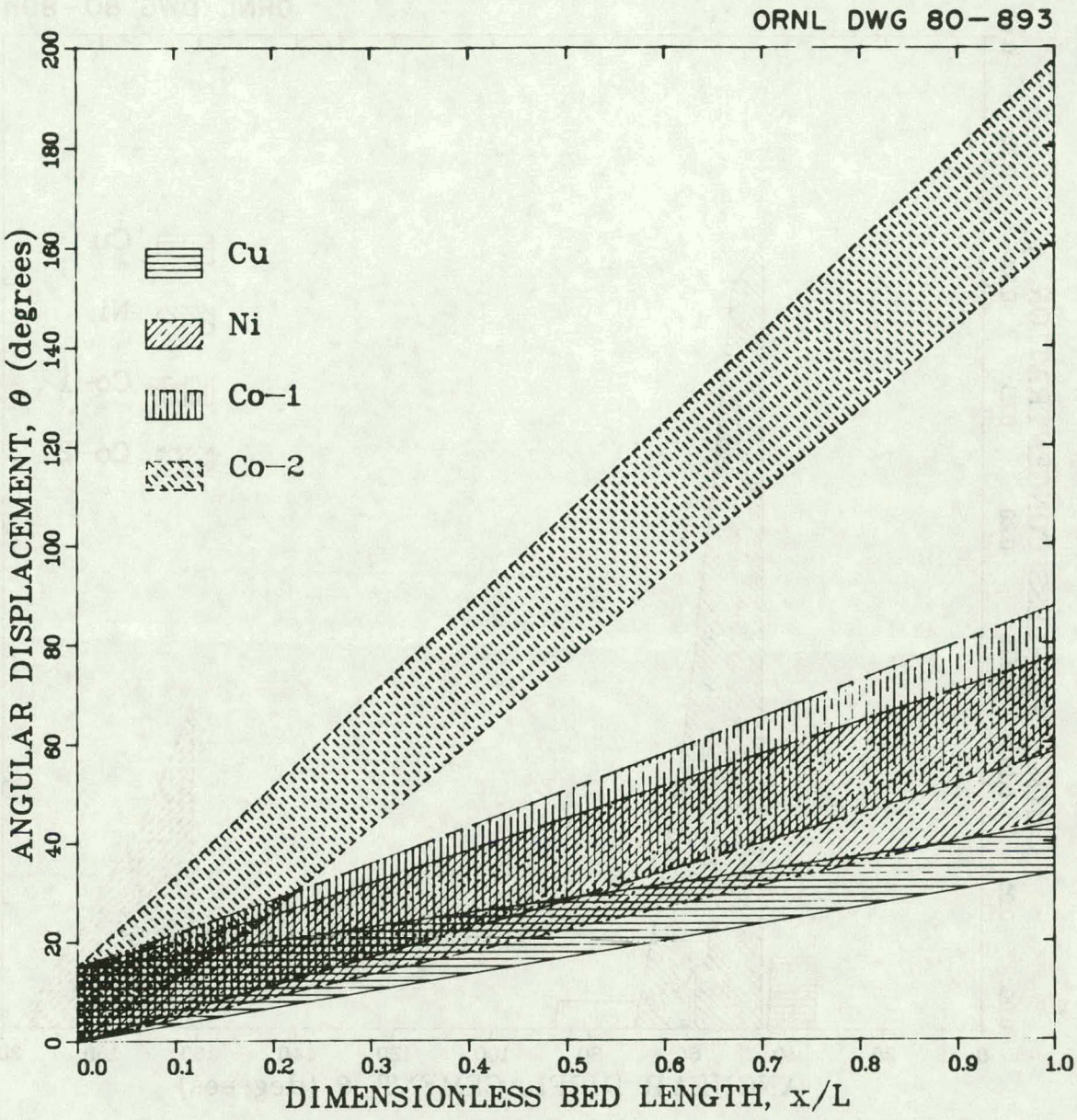

Fig. B.17. Solute bands along the column length for a 38-mm feed bandwidth.

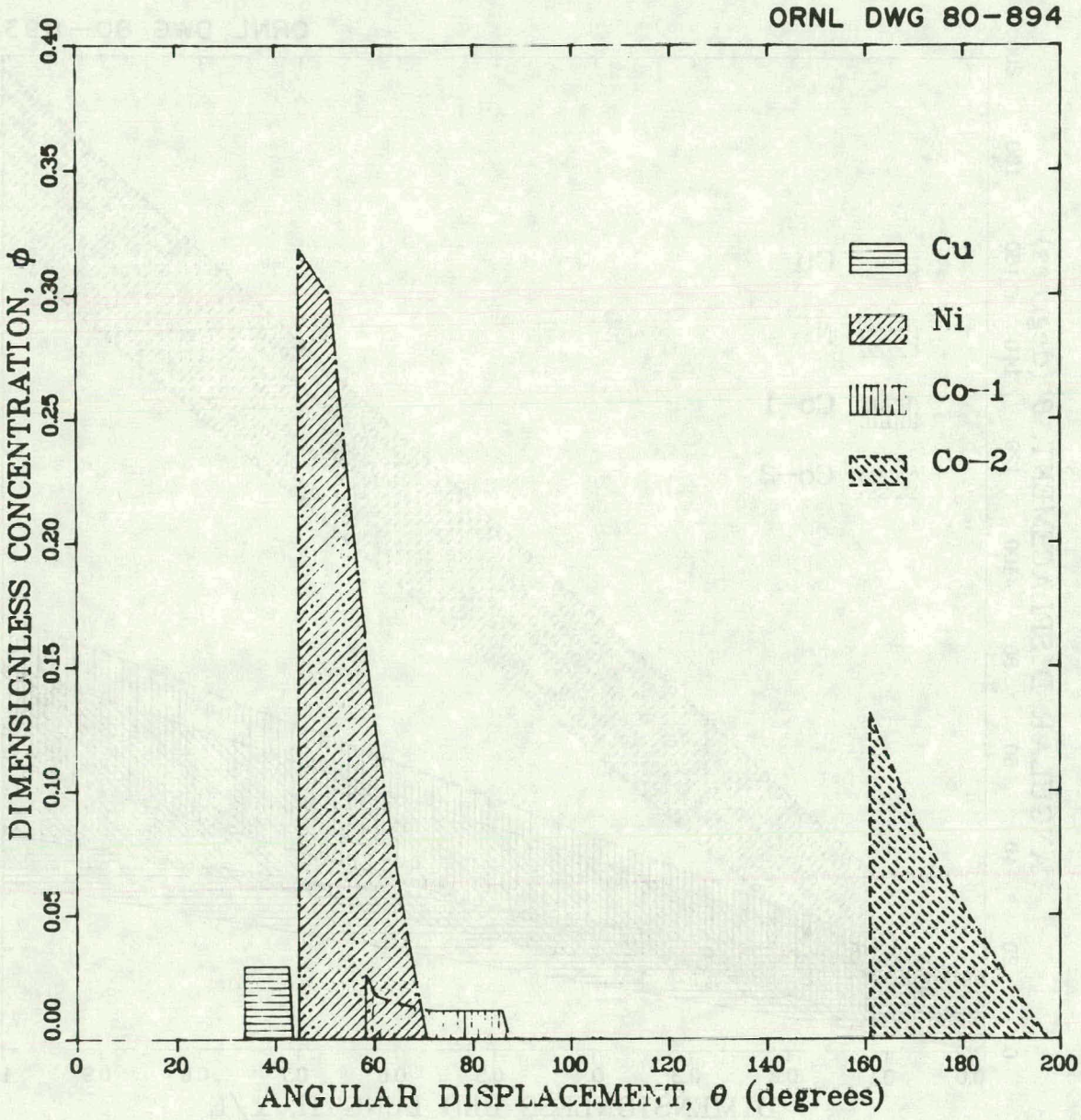

Fig. B.18. Concentration profile at the column exit for a 38-mm feed bandwidth.

8. REFERENCES

1. L. Lapidus and N. Amundson, "Mathematics of Adsorption in Beds. VI. The Effect of Longitudinal Diffusion in Ion Exchange and Chromatographic Columns," J. Phys. Chem. 56, 984 (1952).

2. H. K. Rhee, R. Aris, and N. R. Amundson, "On the Theory of Multicomponent Chromatography," Trans. R. Soc. A267, 419 (1970).

3. R. Aris and N. R. Amundson, AIChE J. 3, 230 (1957).

4. C. D. Scott, R. D. Spence, and W. G. Sisson, "Pressurized Annular Chromatograph for Continuous Separations," J. Chromatogr. 126, 381 (1976).

5. R. Y. Shah, J. H. Austin, and L. M. Burelle, Comprehensive Model for an Annular Continuous Chromatograph, ORNL/MIT-205 (December 1974).

6. R. M. Canon and W. G. Sisson, "Operation of an Improved, Continuous Annular Chromatograph," J. Liq. Chromatogr. 1(4), 427 (1978).

7. R. M. Canon, Section 2.1 in Advanced Technology Section Semiannual Progress Report for the Period Oct. 1, 1977, to Mar. 31, 1978. Volume 2: Engineering Science Programs, ORNL/TM-6377/V2 (July 1980).

THIS PAGE

WAS INTENTIONALLY

LEFT BLANK

ORNL/TM-6706

INTERNAL DISTRIBUTION

1. R. E. Barker
2-6. J. M. Begovich
7-11. R. M. Canon
12. S. D. Clinton
13. R. W. Glass
14. J. R. Hightower
15. F. J. Hurst
16. V. A. Jacobs
17. R. E. Leuze
18. K. J. Notz
19. W. W. Pitt
20. S. E. Shumate
21. W. G. Sisson
22. R. D. Spence
23-27. J. S. Watson
28-29. Central Research Library
30. Document Reference Section
31-32. Laboratory Records
33. Laboratory Records - RC
34. ORNL Patent Office
35. L. Burris, Jr. (consultant)
36. G. R. Choppin (consultant)
37. W. H. Corcoran (consultant)

EXTERNAL DISTRIBUTION

38. R. Aris, Department of Chemical Engineering and Materials Science, University of Minnesota, 421 Washington Avenue, S.E., Minneapolis, MN 55455
39. R. L. Bratzler, Polaroid Corporation, 549 Technology Square, Cambridge, MA 02139
40. J. S. Coleman, Office of Basic Energy Sciences, DOE, Mail Station J-309, GTN, Washington, DC 20545
41. W. J. Haubach, Office of Basic Energy Sciences, DOE, Mail Station J-309, GTN, Washington, DC 20545
42. E. S. Pierce, Office of Basic Energy Sciences, DOE, Mail Station J-309, GTN, Washington, DC 20545
43. F. Dee Stevenson, Office of Basic Energy Sciences, DOE, Mail Station J-309, GTN, Washington, DC 20545
44. M. G. White, Chemical Engineering Department, Georgia Institute of Technology, Atlanta, GA 30332
45. Office of Assistant Manager for Energy Research and Development, DOE-ORO, Oak Ridge, TN 37830
46-72. Technical Information Center, Oak Ridge, TN 37830